arXiv:1901.05905v3 [cond-mat.str-el] 14 Jun 2019

$SU(4)$ topological RVB spin liquid on the square lattice

Olivier Gauthé,[1] Sylvain Capponi,[1] and Didier Poilblanc[1,2]

[1] *Laboratoire de Physique Théorique, Université de Toulouse, CNRS, UPS, France*
[2] *Institute of Theoretical Physics, École Polytechnique Fédérale de Lausanne (EPFL), CH-1015 Lausanne, Switzerland*

(Dated: March 11, 2024)

We generalize the construction of the spin-1/2 SU(2) Resonating Valence Bond (RVB) state to the case of the self-conjugate **6**-representation of SU(4). As for the case of SU(2) [J-Y. Chen and D. Poilblanc, Phys. Rev. B **97**, 161107(R) (2018)], we use the Projected Entangled Pair State (PEPS) formalism to derive a simple (two-dimensional) family of generalized SU(4) RVB states on the square lattice. We show that, when longer-range SU(4)-singlet bonds are included, a local gauge symmetry is broken down from U(1) to $\mathbb{Z}_2$, leading to the emergence of a short-range spin liquid. Evidence for the topological nature of this spin liquid is provided by the investigation of the Renyi entanglement entropy of infinitely-long cylinders and of the modular matrices. Relevance to microscopic models and experiments of ultracold atoms is discussed.

Introduction – Physical systems such as ultracold atoms loaded on two-dimensional (2D) optical lattices [1–3] are ruled by SU(N) symmetry and offer a rich variety of phase diagrams both experimentally and theoretically [4–6]. They constitute a rich playground to investigate quantum spin liquid (SL) phases, where the SU(N) symmetry is not broken [7].

Tensor network (TN) algorithms such as those using the framework of Projected Entangled Pair States (PEPS) have proven extremely efficient to simulate various quantum SU(2) spin models [8–11]. When dealing with spin liquids, it is possible to encode *global* spin-rotation invariance and lattice symmetries directly at the level of a unique site tensor [12, 13] which completely characterizes the quantum state. In addition, topological order can also be encoded via a *local* gauge symmetry of the tensor [14]. These remarkable properties make the PEPS formalism particularly suited to construct simple Ansätze of topological SLs. For example, the Resonating Valence Bond (RVB) state [15] can be written as a PEPS [16] and was proven to be a topological SL belonging to the same $\mathbb{Z}_2$ topological class as the Toric Code [17] (TC), both on the Kagome [18] and on the square lattice [19]. Although the construction can readily be exported to SU(N) for $N > 2$, it has mostly be applied so far to derive a simple Affleck-Kennedy-Lieb-Tasaki (AKLT) trivial (i.e. non-topological) SU(3) liquid [20], as well as a few topological SU(3) liquids [21, 22]. We here construct a family of simple $\mathbb{Z}_2$ topological SU(4) liquids on the square lattice. Our construction is similar to the PEPS construction of spin-1/2 extended RVB states [19], replacing the fundamental irreducible representation (irrep) of SU(2), namely the two-dimensional spin-1/2 irrep, by the self-conjugate **6**-representation of SU(4). This representation can be seen as the Hilbert space of two fermions with four colors; it is represented by a vertical Young tableau of two boxes $\begin{array}{|c|}\hline\\\hline\\\hline\end{array}$ [23]. As for SU(2), the PEPS wavefunction can be viewed as a linear superposition (or "resonance") of short-range singlet bond configurations [15] as seen in Fig. 1 (a). Note that our SU(4) RVB state may not only contains nearest-neighbor (NN) singlet bonds (so-called NN RVB state) but also longer range singlet bonds, including some connecting the *same* sublattice.

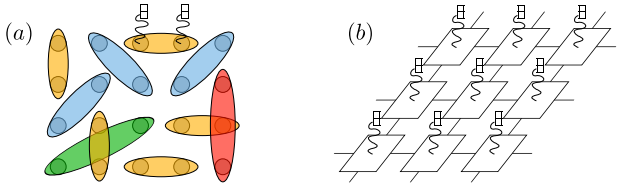

FIG. 1. (a) RVB state defined as a resonance state between SU(4) singlet bond configurations on a 2D square lattice. Singlets (shown as ellipses) are made from two antisymmetric **6**-representations (represented as two box Young tableaus). (b) SU(4) RVB state represented as a 2D PEPS tensor network.

PEPS Ansatz – In order to generalize the square-lattice RVB state [19] to SU(4), one attaches four virtual variables, either **6** or **1** (trivial irrep), to each site along the four lattice directions (see Figs. 2(a,b)), in order to fully cover the square lattice with all possible configurations of $\mathbf{6}-\mathbf{6}$ NN singlet bonds or $\mathbf{1}-\mathbf{1}$ NN "empty" bonds. The entangled RVB state is then obtained by projecting the four virtual states into the physical **6**-representation, on every site, forming the PEPS $|\Psi_{\rm PEPS}\rangle$ represented in Fig. 1 (b). In fact, 16 tensors can be constructed projecting the virtual space $(\mathbf{6}\oplus\mathbf{1})^{\otimes 4}$, of dimension D^4 with $D = 7$, onto the physical SU(4) irrep **6**, of dimension $d = 6$. Rotation-invariant tensors can be classified according to the A_1 and A_2 representations of the point group C_{4v}. The tensor T_0 of Fig. 2(a) representing the NN RVB state is the same as the NN RVB tensor defined for the alternated $\mathbf{6}-\overline{\mathbf{6}}$ representations of SU(6)[24] and has a local A_1 symmetry. The tensors T_1 and T_2 have A_1 symmetry and the tensor T_3 has A_2 symmetry (see Fig. 2(b)). The tensors T_0 and T_1 are actually invariant under any virtual leg permutation (S_4 symmetry group). The most general rotation-invariant tensor describing a short-range RVB state can be written as

$$A = a_0 T_0 + a_1 T_1 + a_2 T_2 + i a_3 T_3, \qquad (1)$$

where the imaginary i factor in front of T_3 is needed to preserve the full lattice symmetry (at the price of break-

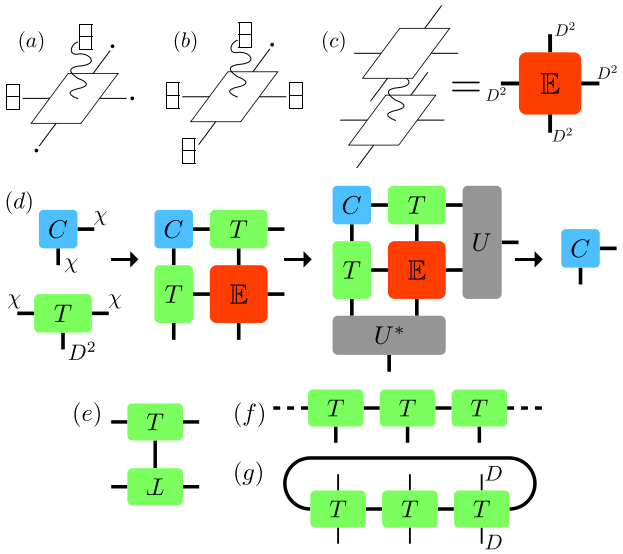

FIG. 2. (a) NN RVB tensor T_0 with only one virtual **6** state. (b) T_1, T_2 and T_3 tensors with three virtual **6** states. (c) In the iPEPS method one constructs first a bi-layer $\mathbb{E} = A \otimes A^*$ tensor by contracting the physical index. (d) Corner Transfer Matrix Renormalization Group (CTMRG) algorithm for a rotation invariant tensor $\mathbb{E}$. A unique corner matrix C and a unique side tensor T are renormalized by adding $\mathbb{E}$ iteratively. (e) Transfer matrix $\mathcal{T} = T \otimes T$. ($f$) $|\Psi_{\rm Env}\rangle$ (infinite) quantum chain obtained by contracting the $\mathbb{E}$ TN on half of the 2D plane (here from top to bottom). (g) σ_b boundary operator on a $N_v = 3$ ring. The D^2 degrees of freedom on each site have been reshaped as $D \times D$.

ing time reversal symmetry). The expressions of these 4 elementary tensors can be found in the supplemental material (SM) [25]. Since two different singlets can be made on a bond, either $\mathbf{6} \otimes \mathbf{6} \to \mathbf{1}$ or $\mathbf{1} \otimes \mathbf{1} \to \mathbf{1}$, there is a one-dimensional family of valid bond projector parametrized by an angle κ, $P(\kappa) = \cos\kappa(\mathcal{P}_{\mathbf{6}\otimes\mathbf{6}} \otimes \mathbb{1}) + \sin\kappa(\mathbb{1} \otimes \mathcal{P}_{\mathbf{1}\otimes\mathbf{1}})$, which are all equivalent up to renormalization of the T_i tensors [26] (for simplicity, we chose $\kappa = \pi/4$). Implicitly, this projector is applied on every bond of the TN (see SM for details [25]).

CTMRG algorithm – In the following we work directly in the thermodynamic limit, i.e. on an infinite 2D lattice, with the "double-layer" TN representing the norm $\langle\Psi_{\rm PEPS}|\Psi_{\rm PEPS}\rangle$ (iPEPS method). The Corner Transfer Matrix Renormalization Group (CTMRG) algorithm [27] is an efficient way to contract the corresponding elementary tensor $\mathbb{E} = A \otimes A^*$ shown in Fig. 2 (c). This procedure involves controlled approximations, using a real space renormalization group technique, depicted in Fig. 2 (d). The infinite-volume environment of any (rectangular) region of space is approximated using an edge tensor T of dimension $\chi \times D^2 \times \chi$ and a corner $\chi \times \chi$ matrix C, where χ is the environment dimension taken as large as possible. C is obtained iteratively by adding tensors $\mathbb{E}$ to the corner, diagonalizing the resulting hermitian matrix and keeping only χ eigenvalues. The exact value of χ has to fit the decomposition of the spectrum into SU(4) multiplets and cannot be fixed arbitrarily. A new tensor T is then computed using the diagonalization basis U. Thanks to lattice rotation invariance, the renormalization process can be performed on one corner only; it is processed until the spectrum of C has converged.

By (approximately) contracting the $\mathbb{E}$ tensor network from infinitely far away on the left and right of the 2D plane, one then ends up with an infinitely long (vertical) two-leg ladder $(T \otimes T)^L$, $L \to \infty$ (where the D^{2L} virtual indices between the two chains of T tensors are contracted). Using Lanczos algorithm, one can extract the two leading eigenvalues λ_1 and λ_2 of the corresponding ladder transfer matrix $\mathcal{T}$ (see Fig. 2(e)) and compute the correlation length ξ of the system from the TM gap Δ as $\Delta = \frac{1}{\xi} = \log\left(\frac{\lambda_1}{\lambda_2}\right)$. Note that the finiteness of the corner dimension χ automatically implies a finite correlation length, so that a finite-χ scaling analysis is necessary. For a short-ranged wavefunction, $\xi(\chi)$ converges exponentially fast towards a finite length ξ_∞. In contrast, for critical $|\Psi_{\rm PEPS}\rangle$ wavefunctions, ξ increases linearly with χ, diverging in the relevant $\chi \to \infty$ limit.

TABLE I. Properties of the four critical PEPS. *Tensors invariant under the larger S_4 symmetric group (see text).

tensor	C_{4v} symmetry	central charge	dimer exponent α
T_0	A_1^*	1	1.75 ± 0.02
T_1	A_1^*	1	1.57 ± 0.15
T_2	A_1	1	1.83 ± 0.08
T_3	A_2	1	1.45 ± 0.11

Critical spin liquids – The four elementary tensors T_0, T_1, T_2 and T_3 define critical states with long-distance correlations. In fact, they can be viewed as Rokhsar-Kilvelson (i.e. equal weight) ground states of quantum dimer models [28], where the "dimers" correspond here either to **6**–**6** (for T_0) or to **1**–**1** (for T_i, $i = 1, 2, 3$) singlet bonds. On bipartite lattices, such as the square lattice, a simple mapping onto a (coarse-grained) height field theory [29] implies algebraically-decaying dimer-dimer correlations $C_d(r) \sim (1/r)^\alpha$ versus distance r. Note that the height representation is linked directly to a local U(1) gauge symmetry of the A tensor. We have directly computed the dimer-dimer correlation functions $C_d(r)$ in these states (using the environment C and T tensors above) and extracted the critical exponents α by fitting the numerical results [25]. The values of α are listed in Table I. Quite notably, RVB wavefunctions can be related to classical interacting dimer models, thus allowing to estimate their critical correlation exponent [30, 31]. Using this equivalence of the T_0 PEPS with the SU(6) RVB state, one predicts $\alpha \simeq 1.64$ which is very close to the value we have measured.

In order to characterize the underlying conformal field theory by its central charge c, we have investigated the entanglement entropy (EE) of the one-dimensional quantum state $|\Psi_{\rm Env}\rangle \in [\mathbb{C}^{D^2}]^{\otimes L}$ made of an infinite ($L \to \infty$) chain $T^{\otimes L}$ of χ-contracted T tensors (see Fig. 2 (f)). The

so-called "environment" EE is computed from the leading eigenvector Σ (reshaped as a $\chi \times \chi$ matrix) of the above $\mathcal{T}$ TM, as $S_{\rm Env} = -\operatorname{Tr}\Sigma^2 \log \Sigma^2$. For a critical wavefunction, the relation $S_{\rm Env} = c/6 \log \xi + S_0$ [32] allows to compute the central charge c (see Fig. 3). We found $c = 1$ in all cases, consistently with the prediction of the height field theory. For T_1, the correlation length stays small even for large χ and we had to include a higher order correction to the fit.

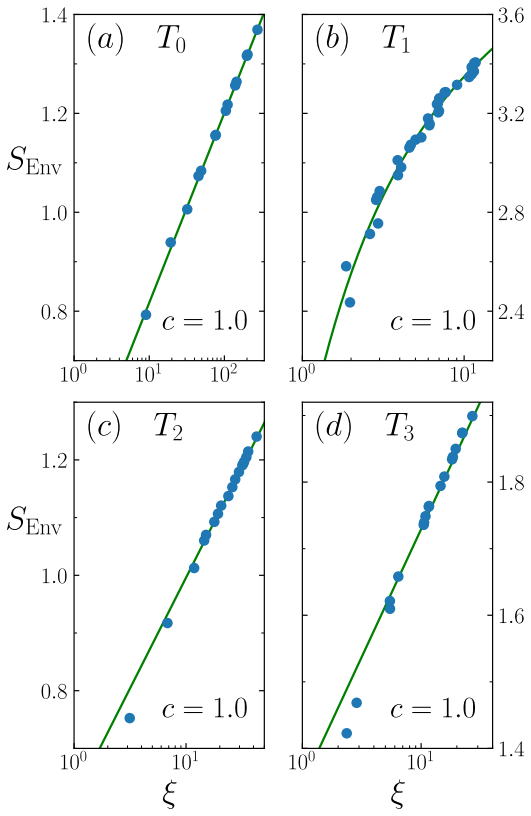

FIG. 3. Environment EE $S_{\rm Env}$ plotted as a function of the logarithm of the correlation length ξ. Linear fits enable to extract the central charge c of the wavefunctions defined by T_0, T_2 and T_3; a higher order correction $a\,\xi^{-b}$ is included for T_1 . We find $c \simeq 1$ in all cases.

Phase diagram – For simplicity, we shall not consider the T_1 tensor any further and restrict to the two-dimensional PEPS family parametrized by two angles θ and ϕ, defining the coefficients of the $A \equiv A(\theta, \phi)$ tensor in Eq. (1) as $a_0 = \cos\phi \sin\theta$, $a_1 = 0$, $a_2 = \cos\phi\cos\theta$ and $a_3 = \sin\phi$. For each elementary tensor, a fix number of dimers – either 1 for T_0 or 3 for T_1, T_2 and T_3 – connect to each site. Hence the number of (fluctuating) dimers cutting a given closed loop is conserved. This means the wavefunction defined by one tensor alone has a U(1) gauge symmetry. For any linear combination of the fundamental tensors with $a_0 \neq 0$, long-range dimers appear and this number of fluctuating dimers is no more constant, but its parity is. Thus U(1) symmetry breaks into $\mathbb{Z}_2$ and we expect the above critical SLs to become

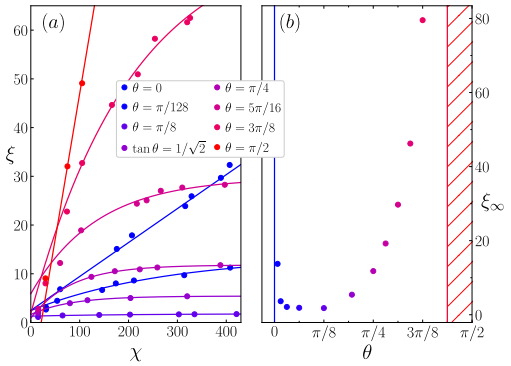

FIG. 4. (a) Correlation length versus environment dimension for $\phi = 0$, and various values of θ interpolating $A(\theta, 0)$ between T_2 ($\theta = 0$) and T_0 ($\theta = \pi/2$). The $\chi \to \infty$ correlation length ξ_∞ (for $\theta \neq 0, \pi/2$) is obtained from an exponential fit $\xi(\chi) = \xi_\infty + a\exp(-\chi/\ell)$. ($b$) Correlation length ξ_∞ versus θ (for $\phi = 0$). The correlation length seems to diverge for $\theta < \pi/2$ (in the vicinity of the NN RVB) in the hashed region. In contrast, no critical region was found in the vicinity of the critical point $\theta = \phi = 0$ (blue line). Note that the correlation length has a minimum around $\theta = \pi/8$.

unstable. As shown in Fig. 4 (a), along the line interpolating between the T_2 and T_0 tensors, one can extract the correlation length from a fit of $\xi(\chi)$ vs χ. As shown in Fig. 4 (b), we found an extended critical region around the NN RVB state. However, a complete scan of the whole two-dimensional phase diagram (see SM [25] for more data) reveals no sign of other extended critical regions in the vicinity of the critical states defined by the T_2 and T_3 tensors.

PEPS bulk-edge correspondence and topological EE – We now turn to the investigation of the topological properties of the short-range SU(4) SL of our phase diagram. For this, we use the bulk-edge correspondence theorem of PEPS [33] applied to an infinitely long (horizontal) cylinder (of finite perimeter N_v) partitioned in two halves by a vertical plane : The reduced density matrix $\rho_{\mathcal{C}} = \operatorname{Tr}_{\bar{\mathcal{C}}} |\Psi_{\rm PEPS}\rangle\langle\Psi_{\rm PEPS}|$ of the half-cylinder $\mathcal{C}$ can be expressed as $\rho_{\mathcal{C}} = U \rho_b U^\dagger$, where ρ_b is a boundary density matrix acting on the virtual space $[\mathbb{C}^D]^{\otimes N_v}$ at the boundary of $\mathcal{C}$ and U is an isometry. Naturally, due to the tensor $\mathbb{Z}_2$ gauge symmetry, ρ_b splits into two $\mathbb{Z}_2$-even and $\mathbb{Z}_2$-odd invariant blocks (normalized separately). Using the CTMRG algorithm, ρ_b can be well approximated by $\rho_b = \sigma_b^2$, where σ_b is the product of (reshaped) edge T tensors shown in Fig. 2 (g), and used to compute Renyi EE defined as $S_q = \frac{1}{1-q} \log \operatorname{Tr}(\rho_b)^q$. Although finite-$\chi$ effects are large for $q > 1$, we have obtained converged results for $q = 1/2$ and $q = 1/3$ [34] (see SM [25] for details). As shown in Fig. 5 for three different PEPS, $S_{1/3}$ versus N_v can be well fitted by a straight line which intersects the vertical axis at a finite value consistent with $-\log 2$, the topological EE expected for a $\mathbb{Z}_2$ SL of the same class as Kitaev's TC [17]. Note the fit in (b) and (c) may be less reliable since N_v remains smaller than ξ.

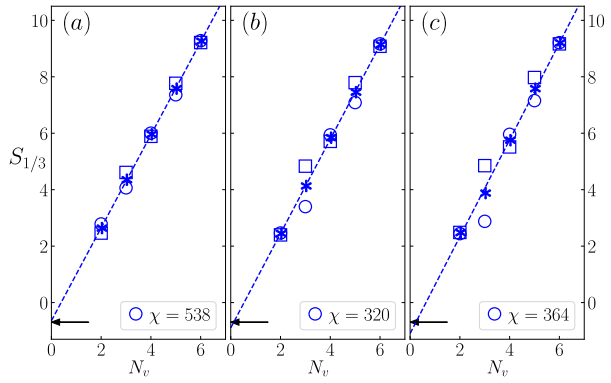

FIG. 5. Renyi entanglement entropies S_q at $q = 1/3$ versus the half-cylinder circumference N_v for PEPS parametrized by (a) $\phi = 0$ and $\theta = \pi/8$, (b) $\phi = 0$ and $\theta = 3\pi/8$, and (c) $\phi = \pi/4$ and $\theta = \pi/2$, obtained at the χ values indicated on the plots. Squares (circles) label the odd (even) sector. The stars stand for the average of the two sectors and the dashed lines are linear fits. The arrow points to the value $-\log 2$.

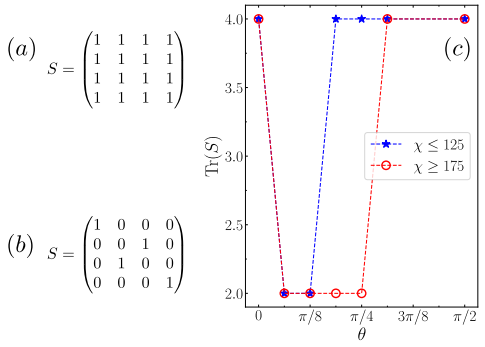

FIG. 6. (*a*) Modular matrix S of a critical or a trivial gapped phase. (*b*) Modular matrix S of a topological phase. (*c*) Trace of the modular matrix S obtained by TRG for $A(\theta, 0)$ versus θ. The value 2 corresponds to a topological phase while 4 implies a trivial phase. We show two sets of data obtained for two ranges of the cut parameter χ and we note that larger χ are needed when the correlation length grows.

However, in (a) $\xi \ll N_v$.

TRG and modular matrices – To obtain further evidence for the topological nature of our family of short-ranged SLs, we have used the Tensor Renormalization Group (TRG) algorithm to compute the S and T modular matrices [35]. At the PEPS tensor level, the $\mathbb{Z}_2$ gauge transformation simply amounts to multiplying by -1 (respectively $+1$) the *virtual* states in the **6** (respectively **1**) irrep, and this gauge symmetry has to be preserved at each TRG iteration [35, 36]. The accuracy of the TRG is also controlled by the maximum number of singular values χ that are kept at each step, always being careful not to cut multiplets. After convergence, we can easily act with elements of the $\mathbb{Z}_2$ group in order to compute the modular matrices [19].

The two modular matrices S and T are actually linked by permutation of the lines. A critical or a trivial gapped phase (a topological phase with $\mathbb{Z}_2$ topological order) is characterized by the modular matrix S shown in Fig. 6(*a*) (Fig. 6(*b*)). The trace of the converged modular matrix S plotted in Fig. 6(*c*) vs θ at fixed $\phi = 0$ shows two sharp transitions revealing the existence of an extended topological SL phase. Note that, when increasing the control parameter χ, the extent of the topological phase gets bigger, in agreement with our previous finding that criticality exists only at $\theta = 0$ and in the close vicinity of $\theta = \pi/2$ (T_0 PEPS).

Conclusion – In summary, we have extended the construction of the family of spin-1/2 SU(2)-invariant RVB states on the square lattice to a new family of SU(4)-symmetric RVB SLs with physical **6**-representation on each site. Physically, such states involve resonance between short-range $\mathbf{6} - \mathbf{6}$ singlets, in close analogy with their SU(2) analogs. Using an exact PEPS representation of these SLs we showed that (i) when singlet dimers are restricted to NN bonds, the SLs are critical, (ii) away from these fine-tuned states (or small region) the SLs have short-range correlations and (iii) exhibit $\mathbb{Z}_2$ topological order. By generalizing Oshikawa's argument [37], one can extend Lieb-Schultz-Mattis-Hastings theorem [38, 39] to conjecture that it is not possible to obtain a unique featureless gapped state for SU(4) model with physical 6-representation on each site [40]. Note that, for complex PEPS (i.e. when the T_3 tensor is included), there is no sign of gapless chiral edge modes.

We believe our topological SL could be observed both in theoretical models and in experiment. On the theory side, the most general SU(4)-invariant NN Hamiltonian in the **6**-representation involves only bilinear and biquadratic interactions [41]. While a pure bilinear model (Heisenberg like) is expected to stabilize an ordered phase [23], early calculations based on projected wavefunctions [41] suggest the existence of a narrow SL region (for a sign of the biquadratic interaction appropriate to a half-filled fermionic Hubbard model [42]), whose exact nature remains unclear. Our topological SL is therefore a good candidate for this phase, although other alternatives like a chiral SL - as for the SU(3) triangular lattice [43] - may exist. Note that SU(4) differs from SU(2) where no SL survives in the case of NN interactions only. This leaves open the possibility of experimental realizations using any ultracold alkaline-earth atoms realizing SU(N) symmetry by simply tuning the number of species [44] to e.g. $N = 4$. Fixing a filling of two particles per site should avoid three-body losses and thus allow controlled experiments.

Acknowledgments. This project is supported by the TNSTRONG ANR-16-CE30-0025 and TNTOP ANR-18-CE30-0026-01 grants (French Research Council). This work was granted access to the HPC resources of CALMIP supercomputing center under the allocation 2018-P1231. We acknowledge inspiring conversations with Fabien Alet, Ji-Yao Chen, Matthieu Mambrini, Frédéric Mila, Román Orús, David Pérez-García, Pierre Pujol, and Keisuke Totsuka.

[1] I. Bloch, "Ultracold quantum gases in optical lattices," Nature Physics **1**, 23 (2005).

[2] M. Lewenstein, A. Sanpera, and V. Ahufinger, *Ultracold Atoms in Optical Lattices: Simulating quantum many-body systems* (Oxford University Press, 2012).

[3] M. A. Cazalilla and A. M. Rey, "Ultracold Fermi gases with emergent SU(N) symmetry," Reports on Progress in Physics **77**, 124401 (2014).

[4] M. A. Cazalilla, A. F. Ho, and M. Ueda, "Ultracold gases of ytterbium: ferromagnetism and Mott states in an SU(6) Fermi system," New Journal of Physics **11**, 103033 (2009).

[5] C. Laflamme, W. Evans, M. Dalmonte, U. Gerber, H. Meja-Daz, W. Bietenholz, U.-J. Wiese, and P. Zoller, "$CP(N-1)$ quantum field theories with alkaline-earth atoms in optical lattices," Annals of Physics **370**, 117 (2016).

[6] S. Capponi, P. Lecheminant, and K. Totsuka, "Phases of one-dimensional SU(N) cold atomic Fermi gasesFrom molecular Luttinger liquids to topological phases," Annals of Physics **367**, 50 (2016).

[7] X.-G. Wen, "Quantum orders and symmetric spin liquids," Phys. Rev. B **65**, 165113 (2002).

[8] D. Poilblanc, N. Schuch, and Ian Affleck, "$SU(2)_1$ chiral edge modes of a critical spin liquid," Phys. Rev. B **93**, 174414 (2016).

[9] D. Poilblanc and M. Mambrini, "Quantum critical phase with infinite projected entangled paired states," Phys. Rev. B **96**, 014414 (2017).

[10] D. Poilblanc, "Investigation of the chiral antiferromagnetic Heisenberg model using projected entangled pair states," Phys. Rev. B **96**, 121118 (2017).

[11] I. Niesen and P. Corboz, "A tensor network study of the complete ground state phase diagram of the spin-1 bilinear-biquadratic Heisenberg model on the square lattice," SciPost Physics **3**, 030 (2017).

[12] M. Mambrini, R. Orús, and D. Poilblanc, "Systematic construction of spin liquids on the square lattice from tensor networks with SU(2) symmetry," Phys. Rev. B **94**, 205124 (2016).

[13] P. Schmoll, S. Singh, M. Rizzi, and R. Orús, "A programming guide for tensor networks with global $SU(2)$ symmetry," arXiv:1809.08180 (2018).

[14] N. Schuch, I. Cirac, and D. Pérez-García, "PEPS as ground states: Degeneracy and topology," Annals of Physics **325**, 2153 (2010).

[15] P. W. Anderson, "The Resonating Valence Bond state in La_2CuO_4 and superconductivity," Science **235**, 1196 (1987).

[16] N. Schuch, D. Poilblanc, J. I. Cirac, and D. Pérez-García, "Resonating valence bond states in the PEPS formalism," Phys. Rev. B **86**, 115108 (2012).

[17] A. Kitaev, "Anyons in an exactly solved model and beyond," Annals of Physics **321**, 2 (2006).

[18] D. Poilblanc, N. Schuch, David Pérez-García, and J. I. Cirac, "Topological and entanglement properties of resonating valence bond wave functions," Phys. Rev. B **86**, 014404 (2012).

[19] J.-Y. Chen and D. Poilblanc, "Topological $\mathbb{Z}_2$ resonating-valence-bond spin liquid on the square lattice," Phys. Rev. B **97**, 161107 (2018).

[20] O. Gauthé and D. Poilblanc, "Entanglement properties of the two-dimensional SU(3) Affleck-Kennedy-Lieb-Tasaki state," Phys. Rev. B **96**, 121115 (2017).

[21] I. Kurečić, L. Vanderstraeten, and N. Schuch, "Gapped SU(3) spin liquid with $\mathbb{Z}_3$ topological order," Phys. Rev. B **99**, 045116 (2019).

[22] X.-Y. Dong, J.-Y. Chen, and H.-H. Tu, "SU(3) trimer resonating-valence-bond state on the square lattice," Phys. Rev. B **98**, 205117 (2018).

[23] F. H. Kim, K. Penc, P. Nataf, and F. Mila, "Linear flavor-wave theory for fully antisymmetric SU(N) irreducible representations," Phys. Rev. B **96**, 205142 (2017).

[24] J.-M. Stéphan, H. Ju, P. Fendley, and R. G. Melko, "Entanglement in gapless resonating-valence-bond states," New Journal of Physics **15**, 015004 (2013).

[25] See the supplementary material for more information.

[26] S. Jiang and Y. Ran, "Symmetric tensor networks and practical simulation algorithms to sharply identify classes of quantum phases distinguishable by short-range physics," Phys. Rev. B **92**, 104414 (2015).

[27] R. Orús and G. Vidal, "Simulation of two-dimensional quantum systems on an infinite lattice revisited: Corner transfer matrix for tensor contraction," Phys. Rev. B **80**, 094403 (2009).

[28] D. S. Rokhsar and Steven A. Kivelson, "Superconductivity and the quantum hard–core dimer gas," Phys. Rev. Lett. **61**, 2376 (1988).

[29] E. Fradkin, D. A. Huse, R. Moessner, V. Oganesyan, and S. L. Sondhi, "Bipartite Rokhsar–Kivelson points and Cantor deconfinement," Phys. Rev. B **69**, 224415 (2004).

[30] K. Damle, D. Dhar, and K. Ramola, "Resonating Valence Bond wave functions and classical interacting dimer models," Phys. Rev. Lett. **108**, 247216 (2012).

[31] F. Alet, Y. Ikhlef, J. L. Jacobsen, G. Misguich, and V. Pasquier, "Classical dimers with aligning interactions on the square lattice," Phys. Rev. E **74**, 041124 (2006).

[32] P. Calabrese and J. Cardy, "Entanglement entropy and quantum field theory," J. Stat. Mech. Theory Exp. **2004**, P06002 (2004).

[33] J. I. Cirac, D. Poilblanc, N. Schuch, and F. Verstraete, "Entanglement spectrum and boundary theories with projected entangled-pair states," Phys. Rev. B **83**, 245134 (2011).

[34] H.-C. Jiang, R. R. P. Singh, and L. Balents, "Accuracy of topological entanglement entropy on finite cylinders," Phys. Rev. Lett. **111**, 107205 (2013).

[35] H. He, H. Moradi, and X.-G. Wen, "Modular matrices as topological order parameter by a gauge-symmetry-preserved tensor renormalization approach," Phys. Rev. B **90**, 205114 (2014).

[36] J.-W. Mei, J.-Y. Chen, H. He, and X.-G. Wen, "Gapped spin liquid with $\mathbb{Z}_2$ topological order for the kagome Heisenberg model," Phys. Rev. B **95**, 235107 (2017).

[37] M. Oshikawa, "Commensurability, excitation gap, and topology in quantum many-particle systems on a periodic lattice," Phys. Rev. Lett. **84**, 1535 (2000).

[38] E. Lieb, T. Schultz, and D. Mattis, "Two soluble models of an antiferromagnetic chain," Annals of Physics **16**, 407 (1961).

[39] M. B. Hastings, "Lieb-Schultz-Mattis in higher dimensions," Phys. Rev. B **69**, 104431 (2004).
[40] K. Totsuka, private communication. Similarly, a non-degenerate featureless gapped ground state is not possible on the square lattice with SU(4) fundamental and antifundamental representation on the two sublattices [45].
[41] A. Paramekanti and J. B. Marston, "SU(N) quantum spin models: a variational wavefunction study," J. Phys.: Condens. Matter **19**, 125215 (2007).
[42] D. Wang, Y. Li, Z. Cai, Z. Zhou, Y. Wang, and C. Wu, "Competing orders in the 2D half-filled SU(2N) Hubbard model through the pinning-field quantum Monte Carlo simulations," Phys. Rev. Lett. **112**, 156403 (2014).
[43] C. Boos, M. Lajkó, P. Nataf, K. Penc, K. P. Schmidt, and F. Mila, "Chiral Mott phase of three-component fermions on the triangular lattice," arXiv:1802.03179 [cond-mat] (2018).
[44] G. Pagano, M. Mancini, G. Cappellini, P. Lombardi, F. Schäfer, H. Hu, X.-J. Liu, J. Catani, C. Sias, M. Inguscio, and L. Fallani, "A one-dimensional liquid of fermions with tunable spin," Nature Physics **10**, 198 (2014).
[45] C.-M. Jian, Z. Bi, and C. Xu, "Lieb-Schultz-Mattis theorem and its generalizations from the perspective of the symmetry-protected topological phase," Phys. Rev. B **97**, 054412 (2018).

arXiv:1901.05905v3 [cond-mat.str-el] 14 Jun 2019

Supplemental Materials: $SU(4)$ topological RVB spin liquid on the square lattice

Olivier Gauthé,[1] Sylvain Capponi,[1] and Didier Poilblanc[1,2]

[1] *Laboratoire de Physique Théorique, Université de Toulouse, CNRS, UPS, France*

[2] *Institute of Theoretical Physics, École Polytechnique Fédérale de Lausanne (EPFL), CH-1015 Lausanne, Switzerland*

(Dated: March 11, 2024)

I. BOND OPERATOR

Two singlets can be made from the two representations **6** or **1** of SU(4). Thus, there exist two linearly independent projectors $(\mathbf{6}\oplus\mathbf{1})^{\otimes 2}\to\mathbf{1}$ on a singlet state, which are matrices of dimension $(49,1)$. We reshape them as matrices $(7,7)$ (which are no more projectors in the mathematical sense) and as explained in the article we choose an angle $\pi/4$ between the projectors $\mathcal{P}_{\mathbf{6}\otimes\mathbf{6}}\otimes\mathbb{1}$ and $\mathbb{1}\otimes\mathcal{P}_{\mathbf{1}\otimes\mathbf{1}}$. The states of the **6**-representation labelled as $|0\rangle$, $|1\rangle$, $|2\rangle$, $|3\rangle$, $|4\rangle$, $|5\rangle$ are defined by their (Cartan) quantum numbers $(1,0,-1)$, $(1,-1,1)$, $(0,-1,0)$, $(0,1,0)$, $(-1,1,-1)$ and $(-1,0,1)$, respectively. The last $|6\rangle$ state corresponds to the **1**-singlet. With this convention of ordering the vectors of the $\mathbf{6}\oplus\mathbf{1}$ representation, the projector we apply reads

$$P = 1/\sqrt{12}\begin{pmatrix} 0 & 0 & 0 & 0 & 0 & 1 & 0\\ 0 & 0 & 0 & 0 & -1 & 0 & 0\\ 0 & 0 & 0 & 1 & 0 & 0 & 0\\ 0 & 0 & 1 & 0 & 0 & 0 & 0\\ 0 & -1 & 0 & 0 & 0 & 0 & 0\\ 1 & 0 & 0 & 0 & 0 & 0 & 0\\ 0 & 0 & 0 & 0 & 0 & 0 & \sqrt{6}\end{pmatrix}. \qquad (1)$$

To avoid dealing explicitly with it in our tensor network algorithm, we absorb P in the definition of the tensor A. More precisely, we consider the square root of P - which is a complex symmetric matrix - and contract it on every physical leg of the initial tensor A as shown in Fig 1 (a). The double layer tensor $\mathbb{E}$ is then computed after this operation is done and it turns out that it also exhibits the same $A_1+\mathrm{i}A_2$ symmetry as the original A tensor.

II. CTMRG ALGORITHM

Thanks to rotation invariance, we renormalize only one corner C instead of doing a full update on the four corners. While diagonalizing the new corner (see Fig. 1 (b)), we obtain a unitary transfer matrix U. This matrix is used to renormalize the edge tensor T, where we add another tensor $\mathbb{E}$ to T as shown in Fig. 1 (c).

III. CORRELATION LENGTHS AND CORRELATION FUNCTIONS

We have computed the (maximum) correlation length ξ of the system using the Lanczos algorithm to diagonalize the approximate transfer matrix. ξ is a function of the corner matrix dimension χ and for a gapped wavefunction, the correlation length converges exponentially to a finite value ξ_∞. For a critical wavefunction, ξ grows linearly with χ as we can see in Fig. 2 for the wavefunctions defined by T_0, T_1, T_2 and T_3. Note that, in that case, the maximum correlation length extracted from the spectrum of the transfer matrix corresponds in fact to the diverging dimer correlation length (see below). Also, for T_1, the slope of ξ vs χ is quite small so that only moderate $\xi\sim 6$ or 7 are accessible even for $\chi\sim 700$. This renders the estimation of the (2+0) central charge and dimer critical exponent more difficult for T_1.

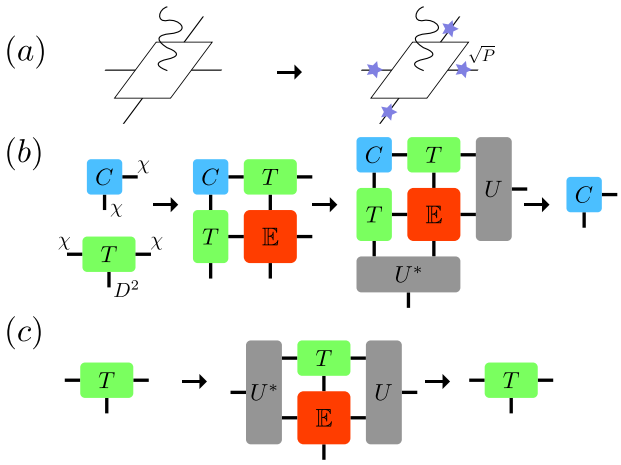

FIG. 1. (a) The square root of the projector on the singlet $\sqrt{P}$ is added to every virtual leg of the initial tensor A. We will then omit this matrix for clarity. Corner Transfer Matrix Renormalization Group (CTMRG) algorithm [1]: (b) Renormalization of the corner matrix C. (c) Renormalization of the side tensor T.

Letting aside the tensor T_1, we have a 2-parameters space parametrized by

$$A(\theta,\phi) = \cos\theta\cos\phi\, T_2 + \sin\theta\cos\phi\, T_0 + i\sin\phi\, T_3 \qquad (2)$$

We show the values of the (maximum) correlation length in this space in Fig 3 for several values of θ and ϕ. The cut parameter χ was taken around 350 but may be slightly different for the different circles. We note that ξ gets larger when A is approaching one of the T_0, T_2 or T_3 corners of the triangular parameter space. It is however unclear on this plot whether there exists any critical region in the vicinity of the three elementary critical wavefunctions. Nevertheless, a finite-χ scaling analysis suggests that there is indeed such a (small) extended critical region around the T_0 corner (see main text).

From the converged C and T tensors one can construct

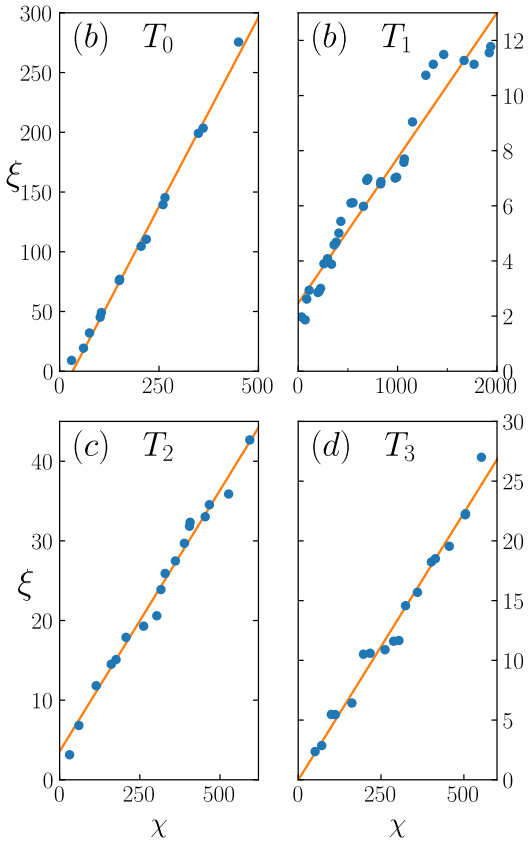

FIG. 2. The maximum correlation length ξ of the system is plotted for the four PEPS given by the elementary tensors T_0, T_1, T_2 and T_3, as a function of the cut parameter χ of the CTMRG algorithm. Fits are linear, which attest that the wavefunctions are critical.

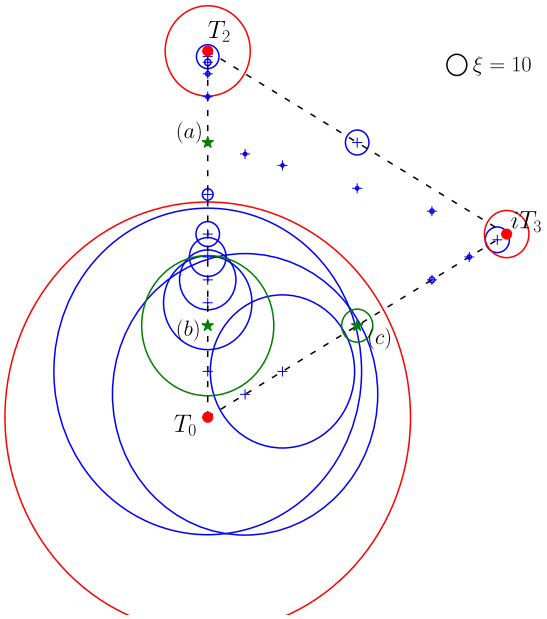

FIG. 3. We consider the (restricted) two-dimensional tensor family given by $A = \cos\theta\cos\phi\, T_2 + \sin\theta\cos\phi\, T_0 + i\sin\phi\, T_3$ and we plot the maximal value of ξ we obtained (the value of χ is not exactly the same for every circle). The red points label the three elementary tensors, the green stars label the points where the boundary entanglement entropy and the entanglement spectrum were computed (see figures (6) and (7)).

the environment of any rectangular subsystem. Using an (infinitely long) strip delimited by two chains of T tensors, we have computed first the expectation value of the observable $\mathbf{S}_i \cdot \mathbf{S}_j$ for all distance $|i-j|$ in the strip direction, as plotted in Fig 4 for the four tensors T_i. We observe a clear exponential decay with a very short "spin" correlation length ξ_S. We have also computed the dimer-dimer correlation function in Fig 5. This observable has long range correlations with algebraic decay, below a finite-χ induced length scale (of the order of the maximum correlation length $\xi(\chi)$). As a consequence, only for large enough χ can one fit the algebraic behavior on a sufficiently large range of distances to obtain accurate values of the critical exponent.

IV. BOUNDARY PROPERTIES

Let us consider the PEPS on an infinitely long cylinder of finite circumference N_v partitioned into two halves. N_v copies of the tensor T are contracted to construct the edges of the two semi-infinite half-cylinders. This vector of dimension D^{2Nv} is then reshaped into a boundary matrix σ_b of shape $D^{Nv} \times D^{N_v}$. The operator $\rho_b = \sigma_b^2$

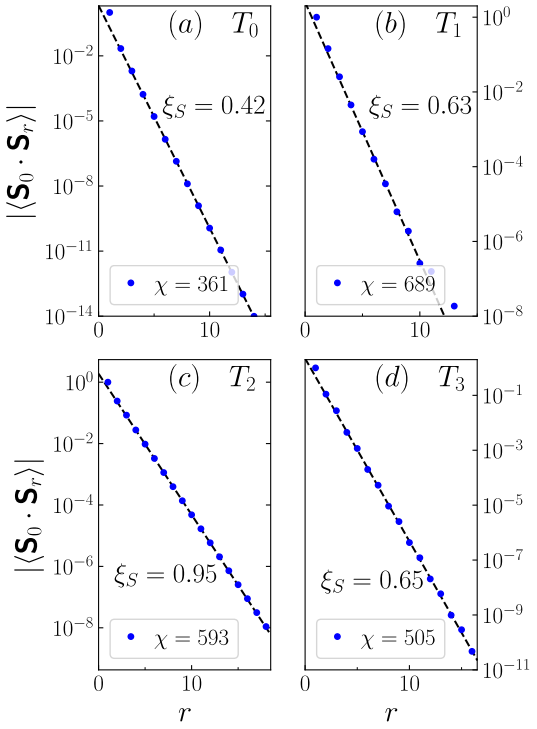

FIG. 4. The "spin" correlation functions are plotted for the four elementary PEPS associated to the T_0, T_1, T_2, and T_3 tensors. We observe an exponential decay with a "spin" correlation length ξ_S.

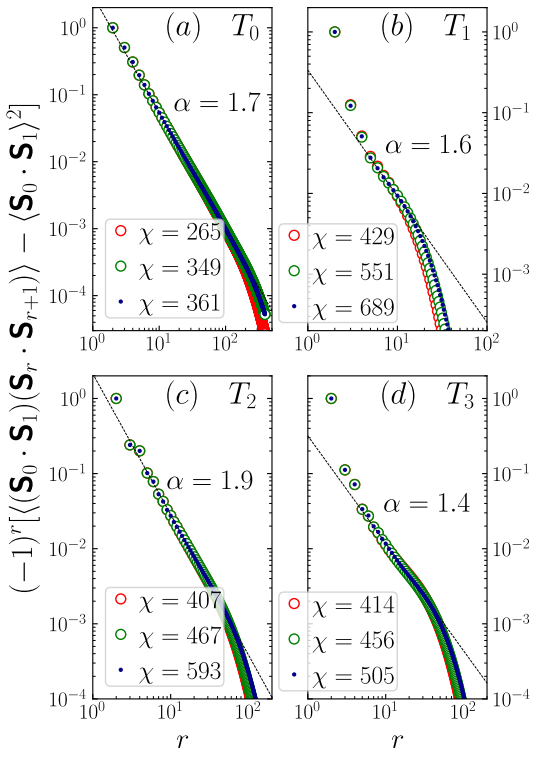

FIG. 5. The dimer-dimer correlation functions are plotted for the four elementary tensors T_0, T_1, T_2, and T_3. We observe a critical behavior with algebraic decay which is cut at large distances by an exponential fall-off. The range of the algebraic behavior extends as χ grows (and would become infinite for $\chi \to \infty$).

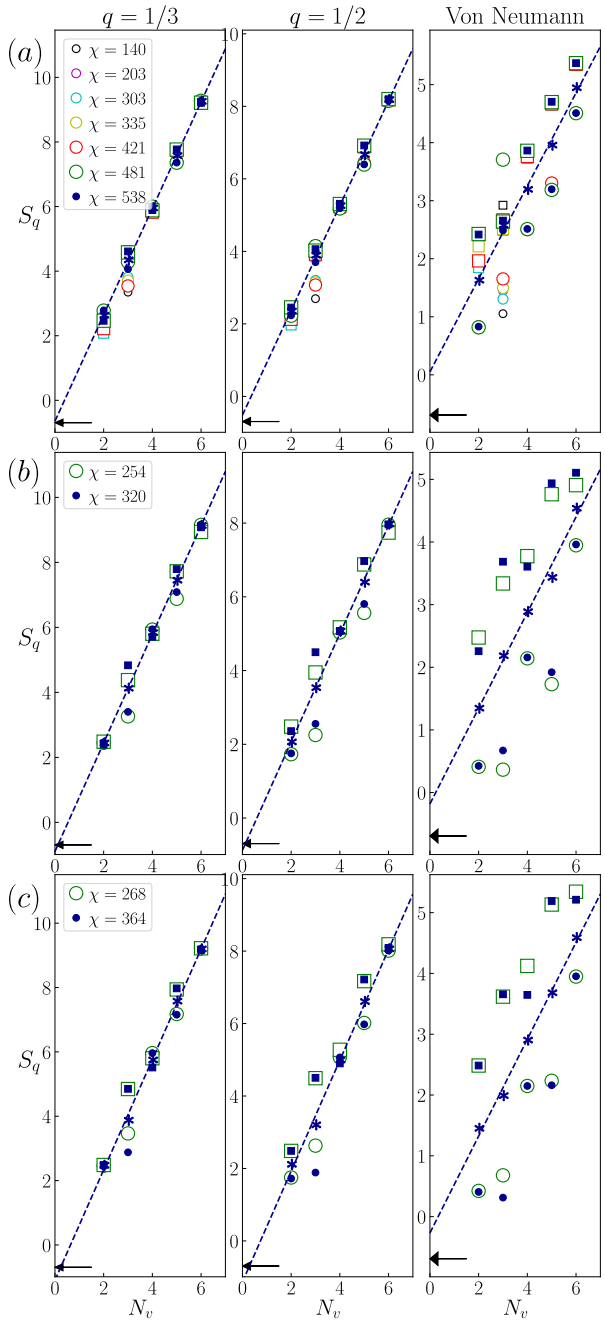

FIG. 6. Renyi entanglement entropies of a partitioned cylinder for the wavefunctions defined in Fig. 3, with respect to the cylinder circumference N_v for $q = 1/3, 1/2$ and 1. The squares label the odd sector and the circles the even one. The stars stand for the average of the two sectors and the dashed lines are their linear fits, the arrow points to the value $-\log 2$.

defined on the one-dimensional virtual space of the cut is related by an isometry (which maps two-dimensions to one-dimension and conserves the spectrum) to the actual reduced density matrix [2] defined by tracing out the physical degrees of freedom of half of the infinite cylinder. The operator ρ_b splits into two $\mathbb{Z}_2$ topological sectors and we normalize those blocks independently to have both traces equal to 1.

The Renyi entanglement entropy associated to the partition of the cylinder is defined from the boundary density matrix ρ_b as $S_q = \log \mathrm{Tr}\, \rho_b^q/(1-q)$, the Von Neumann entropy being the limit $q \to 1$. The entanglement entropy satisfies the area low i.e. it scales with the length of the cut N_v and its sub-leading correction (constant topological entropy) characterizes the topological nature of the SL. We have split the entropy into its two contributions coming from the even and odd topological sectors (note that the definitions of even and odd are exchanged when N_v is odd) in order to observe the $-\log 2$ topological entropy expected for a $\mathbb{Z}_2$ SL. We have computed S_q for three values of the parameter θ and ϕ, labeled in Fig 3: (*a*) $A = \cos(\pi/8)T_2 + \sin(\pi/8)T_0$, (*b*) $A = \cos(3\pi/8)T_2 + \sin(3\pi/8)T_0$, (*c*) $A = \cos(\pi/4)T_0 + i\sin(\pi/4)T_3$ and plotted it for $q = 1/3, 1/2$ and 1 in Fig 6. We note that as q grows, the extrapolation on the vertical axis deviates substantially from the expected $-\log 2$ value, in agreement with Ref. 3.

The entanglement spectrum [4] is the spectrum of the entanglement Hamiltonian $\mathcal{H}$ defined as $\rho_b = \exp(-\mathcal{H})$. The entanglement spectrum is shown in Fig 7 for the three points (*a*), (*b*) and (*c*). The ground state of $\mathcal{H}$ is always an even singlet and the first excitation is an odd **6** irrep. We believe the excitation energy remains finite for

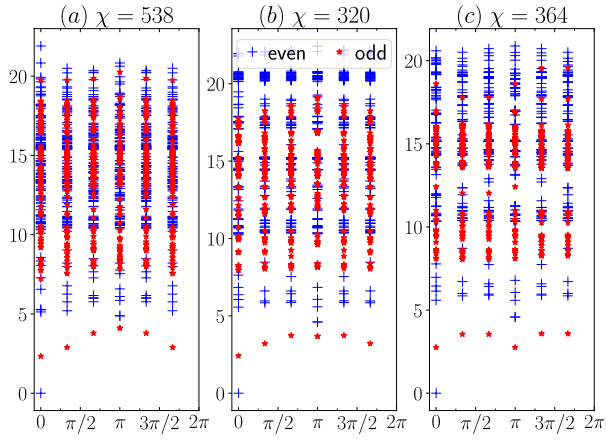

FIG. 7. Entanglement spectrum of a semi-infinite cylinder of circumference $N_v = 6$ with respect to the wavevector along the edge in the two topological even and odd sectors (*a*) $A = \cos(\pi/8)T_2 + \sin(\pi/8)T_0$ with $\chi = 303$ (*b*) $A = \cos(3\pi/8)T_2 + \sin(3\pi/8)T_0$ with $\chi = 254$ (*c*) $A = \cos(\pi/4)T_0 + i\sin(\pi/4)T_3$ with $\chi = 268$ (see Fig. (3)) for the location in the parameter space.

$N_v \to \infty$ i.e. the entanglement spectrum remains *gapped*. The points (*a*) and (*b*) correspond to real wavefunctions and we indeed observe a $k \longleftrightarrow -k$ symmetry in the spectrum associated to time-reversal ($\mathcal{T}$) and parity ($\mathcal{P}$) symmetries. The point (*c*) labels a complex wavefunction with $A_1 + iA_2$ symmetry that breaks $\mathcal{T}$ and $\mathcal{P}$. We observe that the even sector of the entanglement spectrum still exhibits the $k \longleftrightarrow -k$ symmetry, but not the odd sector, which follows a $k \longleftrightarrow \pi - k$ symmetry. We believe this is due to the fact that the product $\mathcal{TP}$ is still preserved. Note also that we have not observed the emergence of gapless chiral edge modes, the entanglement spectrum being probably gapped.

V. TENSOR EXPRESSIONS

For clarity, we give here the coefficients of the *unnormalized* tensors T_i which are integer values. However, the parametrization of the A PEPS tensor involves the T_i tensors normalized with the Frobenius norm. These four tensors are orthogonal for the dot product defined by this norm. We recall that the first index labels the physical variable (varying from 0 to 5) and the four subsequent indices the virtual variables (varying from 0 to 6) on the links (in e.g. clockwise direction).

$T_0[0,0,6,6,6] = 1$	$T_0[0,6,0,0,6] = 1$	$T_0[0,6,6,0,0] = 1$
$T_0[0,6,6,6,0] = 1$	$T_0[1,1,6,6,6] = 1$	$T_0[1,6,1,6,6] = 1$
$T_0[1,6,6,1,6] = 1$	$T_0[1,6,6,6,1] = 1$	$T_0[2,2,6,6,6] = 1$
$T_0[2,6,2,6,6] = 1$	$T_0[2,6,6,2,6] = 1$	$T_0[2,6,6,6,2] = 1$
$T_0[3,3,6,6,6] = 1$	$T_0[3,6,3,6,6] = 1$	$T_0[3,6,6,3,6] = 1$
$T_0[3,6,6,6,3] = 1$	$T_0[4,4,6,6,6] = 1$	$T_0[4,6,4,6,6] = 1$
$T_0[4,6,6,4,6] = 1$	$T_0[4,6,6,6,4] = 1$	$T_0[5,5,6,6,6] = 1$
$T_0[5,6,5,6,6] = 1$	$T_0[5,6,6,5,6] = 1$	$T_0[5,6,6,6,5] = 1$

TABLE I: Tensor T_0 (multiplied by $2\sqrt{6}$).

$T_1[0,0,0,5,6] = 2$	$T_1[0,0,0,6,5] = 2$	$T_1[0,0,1,4,6] = -1$
$T_1[0,0,1,6,4] = -1$	$T_1[0,0,2,3,6] = 1$	$T_1[0,0,2,6,3] = 1$
$T_1[0,0,3,2,6] = 1$	$T_1[0,0,3,6,2] = 1$	$T_1[0,0,4,1,6] = -1$
$T_1[0,0,4,6,1] = -1$	$T_1[0,0,5,0,6] = 2$	$T_1[0,0,5,6,0] = 2$
$T_1[0,0,6,0,5] = 2$	$T_1[0,0,6,1,4] = -1$	$T_1[0,0,6,2,3] = 1$
$T_1[0,0,6,3,2] = 1$	$T_1[0,0,6,4,1] = -1$	$T_1[0,0,6,5,0] = 2$
$T_1[0,1,0,4,6] = -1$	$T_1[0,1,0,6,4] = -1$	$T_1[0,1,4,0,6] = -1$
$T_1[0,1,4,6,0] = -1$	$T_1[0,1,6,0,4] = -1$	$T_1[0,1,6,4,0] = -1$
$T_1[0,2,0,3,6] = 1$	$T_1[0,2,0,6,3] = 1$	$T_1[0,2,3,0,6] = 1$
$T_1[0,2,3,6,0] = 1$	$T_1[0,2,6,0,3] = 1$	$T_1[0,2,6,3,0] = 1$
$T_1[0,3,0,2,6] = 1$	$T_1[0,3,0,6,2] = 1$	$T_1[0,3,2,0,6] = 1$
$T_1[0,3,2,6,0] = 1$	$T_1[0,3,6,0,2] = 1$	$T_1[0,3,6,2,0] = 1$
$T_1[0,4,0,1,6] = -1$	$T_1[0,4,0,6,1] = -1$	$T_1[0,4,1,0,6] = -1$
$T_1[0,4,1,6,0] = -1$	$T_1[0,4,6,0,1] = -1$	$T_1[0,4,6,1,0] = -1$
$T_1[0,5,0,0,6] = 2$	$T_1[0,5,0,6,0] = 2$	$T_1[0,5,6,0,0] = 2$
$T_1[0,6,0,0,5] = 2$	$T_1[0,6,0,1,4] = -1$	$T_1[0,6,0,2,3] = 1$
$T_1[0,6,0,3,2] = 1$	$T_1[0,6,0,4,1] = -1$	$T_1[0,6,0,5,0] = 2$
$T_1[0,6,1,0,4] = -1$	$T_1[0,6,1,4,0] = -1$	$T_1[0,6,2,0,3] = 1$
$T_1[0,6,2,3,0] = 1$	$T_1[0,6,3,0,2] = 1$	$T_1[0,6,3,2,0] = 1$
$T_1[0,6,4,0,1] = -1$	$T_1[0,6,4,1,0] = -1$	$T_1[0,6,5,0,0] = 2$
$T_1[1,0,1,5,6] = 1$	$T_1[1,0,1,6,5] = 1$	$T_1[1,0,5,1,6] = 1$
$T_1[1,0,5,6,1] = 1$	$T_1[1,0,6,1,5] = 1$	$T_1[1,0,6,5,1] = 1$
$T_1[1,1,0,5,6] = 1$	$T_1[1,1,0,6,5] = 1$	$T_1[1,1,1,4,6] = -2$
$T_1[1,1,1,6,4] = -2$	$T_1[1,1,2,3,6] = 1$	$T_1[1,1,2,6,3] = 1$
$T_1[1,1,3,2,6] = 1$	$T_1[1,1,3,6,2] = 1$	$T_1[1,1,4,1,6] = -2$
$T_1[1,1,4,6,1] = -2$	$T_1[1,1,5,0,6] = 1$	$T_1[1,1,5,6,0] = 1$
$T_1[1,1,6,0,5] = 1$	$T_1[1,1,6,1,4] = -2$	$T_1[1,1,6,2,3] = 1$
$T_1[1,1,6,3,2] = 1$	$T_1[1,1,6,4,1] = -2$	$T_1[1,1,6,5,0] = 1$
$T_1[1,2,1,3,6] = 1$	$T_1[1,2,1,6,3] = 1$	$T_1[1,2,3,1,6] = 1$
$T_1[1,2,3,6,1] = 1$	$T_1[1,2,6,1,3] = 1$	$T_1[1,2,6,3,1] = 1$
$T_1[1,3,1,2,6] = 1$	$T_1[1,3,1,6,2] = 1$	$T_1[1,3,2,1,6] = 1$
$T_1[1,3,2,6,1] = 1$	$T_1[1,3,6,1,2] = 1$	$T_1[1,3,6,2,1] = 1$
$T_1[1,4,1,1,6] = -2$	$T_1[1,4,1,6,1] = -2$	$T_1[1,4,6,1,1] = -2$
$T_1[1,5,0,1,6] = 1$	$T_1[1,5,0,6,1] = 1$	$T_1[1,5,1,0,6] = 1$
$T_1[1,5,1,6,0] = 1$	$T_1[1,5,6,0,1] = 1$	$T_1[1,5,6,1,0] = 1$
$T_1[1,6,0,1,5] = 1$	$T_1[1,6,0,5,1] = 1$	$T_1[1,6,1,0,5] = 1$
$T_1[1,6,1,1,4] = -2$	$T_1[1,6,1,2,3] = 1$	$T_1[1,6,1,3,2] = 1$
$T_1[1,6,1,4,1] = -2$	$T_1[1,6,1,5,0] = 1$	$T_1[1,6,2,1,3] = 1$
$T_1[1,6,2,3,1] = 1$	$T_1[1,6,3,1,2] = 1$	$T_1[1,6,3,2,1] = 1$
$T_1[1,6,4,1,1] = -2$	$T_1[1,6,5,0,1] = 1$	$T_1[1,6,5,1,0] = 1$
$T_1[2,0,2,5,6] = 1$	$T_1[2,0,2,6,5] = 1$	$T_1[2,0,5,2,6] = 1$
$T_1[2,0,5,6,2] = 1$	$T_1[2,0,6,2,5] = 1$	$T_1[2,0,6,5,2] = 1$
$T_1[2,1,2,4,6] = -1$	$T_1[2,1,2,6,4] = -1$	$T_1[2,1,4,2,6] = -1$
$T_1[2,1,4,6,2] = -1$	$T_1[2,1,6,2,4] = -1$	$T_1[2,1,6,4,2] = -1$
$T_1[2,2,0,5,6] = 1$	$T_1[2,2,0,6,5] = 1$	$T_1[2,2,1,4,6] = -1$
$T_1[2,2,1,6,4] = -1$	$T_1[2,2,2,3,6] = 2$	$T_1[2,2,2,6,3] = 2$
$T_1[2,2,3,2,6] = 2$	$T_1[2,2,3,6,2] = 2$	$T_1[2,2,4,1,6] = -1$
$T_1[2,2,4,6,1] = -1$	$T_1[2,2,5,0,6] = 1$	$T_1[2,2,5,6,0] = 1$
$T_1[2,2,6,0,5] = 1$	$T_1[2,2,6,1,4] = -1$	$T_1[2,2,6,2,3] = 2$
$T_1[2,2,6,3,2] = 2$	$T_1[2,2,6,4,1] = -1$	$T_1[2,2,6,5,0] = 1$
$T_1[2,3,2,2,6] = 2$	$T_1[2,3,2,6,2] = 2$	$T_1[2,3,6,2,2] = 2$
$T_1[2,4,1,2,6] = -1$	$T_1[2,4,1,6,2] = -1$	$T_1[2,4,2,1,6] = -1$
$T_1[2,4,2,6,1] = -1$	$T_1[2,4,6,1,2] = -1$	$T_1[2,4,6,2,1] = -1$
$T_1[2,5,0,2,6] = 1$	$T_1[2,5,0,6,2] = 1$	$T_1[2,5,2,0,6] = 1$
$T_1[2,5,2,6,0] = 1$	$T_1[2,5,6,0,2] = 1$	$T_1[2,5,6,2,0] = 1$
$T_1[2,6,0,2,5] = 1$	$T_1[2,6,0,5,2] = 1$	$T_1[2,6,1,2,4] = -1$
$T_1[2,6,1,4,2] = -1$	$T_1[2,6,2,0,5] = 1$	$T_1[2,6,2,1,4] = -1$
$T_1[2,6,2,2,3] = 2$	$T_1[2,6,2,3,2] = 2$	$T_1[2,6,2,4,1] = -1$
$T_1[2,6,2,5,0] = 1$	$T_1[2,6,3,2,2] = 2$	$T_1[2,6,4,1,2] = -1$
$T_1[2,6,4,2,1] = -1$	$T_1[2,6,5,0,2] = 1$	$T_1[2,6,5,2,0] = 1$
$T_1[3,0,3,5,6] = 1$	$T_1[3,0,3,6,5] = 1$	$T_1[3,0,5,3,6] = 1$
$T_1[3,0,5,6,3] = 1$	$T_1[3,0,6,3,5] = 1$	$T_1[3,0,6,5,3] = 1$
$T_1[3,1,3,4,6] = -1$	$T_1[3,1,3,6,4] = -1$	$T_1[3,1,4,3,6] = -1$

$T_1[3,1,4,6,3] = -1$	$T_1[3,1,6,3,4] = -1$	$T_1[3,1,6,4,3] = -1$
$T_1[3,2,3,3,6] = 2$	$T_1[3,2,3,6,3] = 2$	$T_1[3,2,6,3,3] = 2$
$T_1[3,3,0,5,6] = 1$	$T_1[3,3,0,6,5] = 1$	$T_1[3,3,1,4,6] = -1$
$T_1[3,3,1,6,4] = -1$	$T_1[3,3,2,3,6] = 2$	$T_1[3,3,2,6,3] = 2$
$T_1[3,3,3,2,6] = 2$	$T_1[3,3,3,6,2] = 2$	$T_1[3,3,4,1,6] = -1$
$T_1[3,3,4,6,1] = -1$	$T_1[3,3,5,0,6] = 1$	$T_1[3,3,5,6,0] = 1$
$T_1[3,3,6,0,5] = 1$	$T_1[3,3,6,1,4] = -1$	$T_1[3,3,6,2,3] = 2$
$T_1[3,3,6,3,2] = 2$	$T_1[3,3,6,4,1] = -1$	$T_1[3,3,6,5,0] = 1$
$T_1[3,4,1,3,6] = -1$	$T_1[3,4,1,6,3] = -1$	$T_1[3,4,3,1,6] = -1$
$T_1[3,4,3,6,1] = -1$	$T_1[3,4,6,1,3] = -1$	$T_1[3,4,6,3,1] = -1$
$T_1[3,5,0,3,6] = 1$	$T_1[3,5,0,6,3] = 1$	$T_1[3,5,3,0,6] = 1$
$T_1[3,5,3,6,0] = 1$	$T_1[3,5,6,0,3] = 1$	$T_1[3,5,6,3,0] = 1$
$T_1[3,6,0,3,5] = 1$	$T_1[3,6,0,5,3] = 1$	$T_1[3,6,1,3,4] = -1$
$T_1[3,6,1,4,3] = -1$	$T_1[3,6,2,3,3] = 2$	$T_1[3,6,3,0,5] = 1$
$T_1[3,6,3,1,4] = -1$	$T_1[3,6,3,2,3] = 2$	$T_1[3,6,3,3,2] = 2$
$T_1[3,6,3,4,1] = -1$	$T_1[3,6,3,5,0] = 1$	$T_1[3,6,4,1,3] = -1$
$T_1[3,6,4,3,1] = -1$	$T_1[3,6,5,0,3] = 1$	$T_1[3,6,5,3,0] = 1$
$T_1[4,0,4,5,6] = 1$	$T_1[4,0,4,6,5] = 1$	$T_1[4,0,5,4,6] = 1$
$T_1[4,0,5,6,4] = 1$	$T_1[4,0,6,4,5] = 1$	$T_1[4,0,6,5,4] = 1$
$T_1[4,1,4,4,6] = -2$	$T_1[4,1,4,6,4] = -2$	$T_1[4,1,6,4,4] = -2$
$T_1[4,2,3,4,6] = 1$	$T_1[4,2,3,6,4] = 1$	$T_1[4,2,4,3,6] = 1$
$T_1[4,2,4,6,3] = 1$	$T_1[4,2,6,3,4] = 1$	$T_1[4,2,6,4,3] = 1$
$T_1[4,3,2,4,6] = 1$	$T_1[4,3,2,6,4] = 1$	$T_1[4,3,4,2,6] = 1$
$T_1[4,3,4,6,2] = 1$	$T_1[4,3,6,2,4] = 1$	$T_1[4,3,6,4,2] = 1$
$T_1[4,4,0,5,6] = 1$	$T_1[4,4,0,6,5] = 1$	$T_1[4,4,1,4,6] = -2$
$T_1[4,4,1,6,4] = -2$	$T_1[4,4,2,3,6] = 1$	$T_1[4,4,2,6,3] = 1$
$T_1[4,4,3,2,6] = 1$	$T_1[4,4,3,6,2] = 1$	$T_1[4,4,4,1,6] = -2$
$T_1[4,4,4,6,1] = -2$	$T_1[4,4,5,0,6] = 1$	$T_1[4,4,5,6,0] = 1$
$T_1[4,4,6,0,5] = 1$	$T_1[4,4,6,1,4] = -2$	$T_1[4,4,6,2,3] = 1$
$T_1[4,4,6,3,2] = 1$	$T_1[4,4,6,4,1] = -2$	$T_1[4,4,6,5,0] = 1$
$T_1[4,5,0,4,6] = 1$	$T_1[4,5,0,6,4] = 1$	$T_1[4,5,4,0,6] = 1$
$T_1[4,5,4,6,0] = 1$	$T_1[4,5,6,0,4] = 1$	$T_1[4,5,6,4,0] = 1$
$T_1[4,6,0,4,5] = 1$	$T_1[4,6,0,5,4] = 1$	$T_1[4,6,1,4,4] = -2$
$T_1[4,6,2,3,4] = 1$	$T_1[4,6,2,4,3] = 1$	$T_1[4,6,3,2,4] = 1$
$T_1[4,6,3,4,2] = 1$	$T_1[4,6,4,0,5] = 1$	$T_1[4,6,4,1,4] = -2$
$T_1[4,6,4,2,3] = 1$	$T_1[4,6,4,3,2] = 1$	$T_1[4,6,4,4,1] = -2$
$T_1[4,6,4,5,0] = 1$	$T_1[4,6,5,0,4] = 1$	$T_1[4,6,5,4,0] = 1$
$T_1[5,0,5,5,6] = 2$	$T_1[5,0,5,6,5] = 2$	$T_1[5,0,6,5,5] = 2$
$T_1[5,1,4,5,6] = -1$	$T_1[5,1,4,6,5] = -1$	$T_1[5,1,5,4,6] = -1$
$T_1[5,1,5,6,4] = -1$	$T_1[5,1,6,4,5] = -1$	$T_1[5,1,6,5,4] = -1$
$T_1[5,2,3,5,6] = 1$	$T_1[5,2,3,6,5] = 1$	$T_1[5,2,5,3,6] = 1$
$T_1[5,2,5,6,3] = 1$	$T_1[5,2,6,3,5] = 1$	$T_1[5,2,6,5,3] = 1$
$T_1[5,3,2,5,6] = 1$	$T_1[5,3,2,6,5] = 1$	$T_1[5,3,5,2,6] = 1$
$T_1[5,3,5,6,2] = 1$	$T_1[5,3,6,2,5] = 1$	$T_1[5,3,6,5,2] = 1$
$T_1[5,4,1,5,6] = -1$	$T_1[5,4,1,6,5] = -1$	$T_1[5,4,5,1,6] = -1$
$T_1[5,4,5,6,1] = -1$	$T_1[5,4,6,1,5] = -1$	$T_1[5,4,6,5,1] = -1$
$T_1[5,5,0,5,6] = 2$	$T_1[5,5,0,6,5] = 2$	$T_1[5,5,1,4,6] = -1$
$T_1[5,5,1,6,4] = -1$	$T_1[5,5,2,3,6] = 1$	$T_1[5,5,2,6,3] = 1$
$T_1[5,5,3,2,6] = 1$	$T_1[5,5,3,6,2] = 1$	$T_1[5,5,4,1,6] = -1$
$T_1[5,5,4,6,1] = -1$	$T_1[5,5,5,0,6] = 2$	$T_1[5,5,5,6,0] = 2$
$T_1[5,5,6,0,5] = 2$	$T_1[5,5,6,1,4] = -1$	$T_1[5,5,6,2,3] = 1$
$T_1[5,5,6,3,2] = 1$	$T_1[5,5,6,4,1] = -1$	$T_1[5,5,6,5,0] = 2$
$T_1[5,6,0,5,5] = 2$	$T_1[5,6,1,4,5] = -1$	$T_1[5,6,1,5,4] = -1$
$T_1[5,6,2,3,5] = 1$	$T_1[5,6,2,5,3] = 1$	$T_1[5,6,3,2,5] = 1$
$T_1[5,6,3,5,2] = 1$	$T_1[5,6,4,1,5] = -1$	$T_1[5,6,4,5,1] = -1$
$T_1[5,6,5,0,5] = 2$	$T_1[5,6,5,1,4] = -1$	$T_1[5,6,5,2,3] = 1$
$T_1[5,6,5,3,2] = 1$	$T_1[5,6,5,4,1] = -1$	$T_1[5,6,5,5,0] = 2$

TABLE II: Tensor T_1 (multiplied by 24).

$T_2[0,0,0,5,6] = -1$	$T_2[0,0,0,6,5] = -1$	$T_2[0,0,1,4,6] = -1$
$T_2[0,0,1,6,4] = 2$	$T_2[0,0,2,3,6] = 1$	$T_2[0,0,2,6,3] = -2$
$T_2[0,0,3,2,6] = 1$	$T_2[0,0,3,6,2] = -2$	$T_2[0,0,4,1,6] = -1$
$T_2[0,0,4,6,1] = 2$	$T_2[0,0,5,0,6] = 2$	$T_2[0,0,5,6,0] = -1$
$T_2[0,0,6,0,5] = 2$	$T_2[0,0,6,1,4] = -1$	$T_2[0,0,6,2,3] = 1$
$T_2[0,0,6,3,2] = 1$	$T_2[0,0,6,4,1] = -1$	$T_2[0,0,6,5,0] = -1$
$T_2[0,1,0,4,6] = 2$	$T_2[0,1,0,6,4] = -1$	$T_2[0,1,4,0,6] = -1$
$T_2[0,1,4,6,0] = -1$	$T_2[0,1,6,0,4] = -1$	$T_2[0,1,6,4,0] = 2$
$T_2[0,2,0,3,6] = -2$	$T_2[0,2,0,6,3] = 1$	$T_2[0,2,3,0,6] = 1$
$T_2[0,2,3,6,0] = 1$	$T_2[0,2,6,0,3] = 1$	$T_2[0,2,6,3,0] = -2$
$T_2[0,3,0,2,6] = -2$	$T_2[0,3,0,6,2] = 1$	$T_2[0,3,2,0,6] = 1$
$T_2[0,3,2,6,0] = 1$	$T_2[0,3,6,0,2] = 1$	$T_2[0,3,6,2,0] = -2$
$T_2[0,4,0,1,6] = 2$	$T_2[0,4,0,6,1] = -1$	$T_2[0,4,1,0,6] = -1$
$T_2[0,4,1,6,0] = -1$	$T_2[0,4,6,0,1] = -1$	$T_2[0,4,6,1,0] = 2$
$T_2[0,5,0,0,6] = -1$	$T_2[0,5,0,6,0] = 2$	$T_2[0,5,6,0,0] = -1$
$T_2[0,6,0,0,5] = -1$	$T_2[0,6,0,1,4] = -1$	$T_2[0,6,0,2,3] = 1$
$T_2[0,6,0,3,2] = 1$	$T_2[0,6,0,4,1] = -1$	$T_2[0,6,0,5,0] = 2$
$T_2[0,6,1,0,4] = 2$	$T_2[0,6,1,4,0] = -1$	$T_2[0,6,2,0,3] = -2$
$T_2[0,6,2,3,0] = 1$	$T_2[0,6,3,0,2] = -2$	$T_2[0,6,3,2,0] = 1$
$T_2[0,6,4,0,1] = 2$	$T_2[0,6,4,1,0] = -1$	$T_2[0,6,5,0,0] = -1$
$T_2[1,0,1,5,6] = -2$	$T_2[1,0,1,6,5] = 1$	$T_2[1,0,5,1,6] = 1$
$T_2[1,0,5,6,1] = 1$	$T_2[1,0,6,1,5] = 1$	$T_2[1,0,6,5,1] = -2$
$T_2[1,1,0,5,6] = 1$	$T_2[1,1,0,6,5] = -2$	$T_2[1,1,1,4,6] = 1$
$T_2[1,1,1,6,4] = 1$	$T_2[1,1,2,3,6] = 1$	$T_2[1,1,2,6,3] = -2$
$T_2[1,1,3,2,6] = 1$	$T_2[1,1,3,6,2] = -2$	$T_2[1,1,4,1,6] = -2$
$T_2[1,1,4,6,1] = 1$	$T_2[1,1,5,0,6] = 1$	$T_2[1,1,5,6,0] = -2$
$T_2[1,1,6,0,5] = 1$	$T_2[1,1,6,1,4] = -2$	$T_2[1,1,6,2,3] = 1$
$T_2[1,1,6,3,2] = 1$	$T_2[1,1,6,4,1] = 1$	$T_2[1,1,6,5,0] = 1$
$T_2[1,2,1,3,6] = -2$	$T_2[1,2,1,6,3] = 1$	$T_2[1,2,3,1,6] = 1$
$T_2[1,2,3,6,1] = 1$	$T_2[1,2,6,1,3] = 1$	$T_2[1,2,6,3,1] = -2$
$T_2[1,3,1,2,6] = -2$	$T_2[1,3,1,6,2] = 1$	$T_2[1,3,2,1,6] = 1$
$T_2[1,3,2,6,1] = 1$	$T_2[1,3,6,1,2] = 1$	$T_2[1,3,6,2,1] = -2$
$T_2[1,4,1,1,6] = 1$	$T_2[1,4,1,6,1] = -2$	$T_2[1,4,6,1,1] = 1$
$T_2[1,5,0,1,6] = 1$	$T_2[1,5,0,6,1] = 1$	$T_2[1,5,1,0,6] = -2$
$T_2[1,5,1,6,0] = 1$	$T_2[1,5,6,0,1] = -2$	$T_2[1,5,6,1,0] = 1$
$T_2[1,6,0,1,5] = -2$	$T_2[1,6,0,5,1] = 1$	$T_2[1,6,1,0,5] = 1$
$T_2[1,6,1,1,4] = 1$	$T_2[1,6,1,2,3] = 1$	$T_2[1,6,1,3,2] = 1$
$T_2[1,6,1,4,1] = -2$	$T_2[1,6,1,5,0] = 1$	$T_2[1,6,2,1,3] = -2$
$T_2[1,6,2,3,1] = 1$	$T_2[1,6,3,1,2] = -2$	$T_2[1,6,3,2,1] = 1$
$T_2[1,6,4,1,1] = 1$	$T_2[1,6,5,0,1] = 1$	$T_2[1,6,5,1,0] = -2$
$T_2[2,0,2,5,6] = -2$	$T_2[2,0,2,6,5] = 1$	$T_2[2,0,5,2,6] = 1$
$T_2[2,0,5,6,2] = 1$	$T_2[2,0,6,2,5] = 1$	$T_2[2,0,6,5,2] = -2$
$T_2[2,1,2,4,6] = 2$	$T_2[2,1,2,6,4] = -1$	$T_2[2,1,4,2,6] = -1$
$T_2[2,1,4,6,2] = -1$	$T_2[2,1,6,2,4] = -1$	$T_2[2,1,6,4,2] = 2$
$T_2[2,2,0,5,6] = 1$	$T_2[2,2,0,6,5] = -2$	$T_2[2,2,1,4,6] = -1$
$T_2[2,2,1,6,4] = 2$	$T_2[2,2,2,3,6] = -1$	$T_2[2,2,2,6,3] = -1$
$T_2[2,2,3,2,6] = 2$	$T_2[2,2,3,6,2] = -1$	$T_2[2,2,4,1,6] = -1$
$T_2[2,2,4,6,1] = 2$	$T_2[2,2,5,0,6] = 1$	$T_2[2,2,5,6,0] = -2$
$T_2[2,2,6,0,5] = 1$	$T_2[2,2,6,1,4] = -1$	$T_2[2,2,6,2,3] = 2$
$T_2[2,2,6,3,2] = -1$	$T_2[2,2,6,4,1] = -1$	$T_2[2,2,6,5,0] = 1$
$T_2[2,3,2,2,6] = -1$	$T_2[2,3,2,6,2] = 2$	$T_2[2,3,6,2,2] = -1$
$T_2[2,4,1,2,6] = -1$	$T_2[2,4,1,6,2] = -1$	$T_2[2,4,2,1,6] = 2$
$T_2[2,4,2,6,1] = -1$	$T_2[2,4,6,1,2] = 2$	$T_2[2,4,6,2,1] = -1$
$T_2[2,5,0,2,6] = 1$	$T_2[2,5,0,6,2] = 1$	$T_2[2,5,2,0,6] = -2$
$T_2[2,5,2,6,0] = 1$	$T_2[2,5,6,0,2] = -2$	$T_2[2,5,6,2,0] = 1$
$T_2[2,6,0,2,5] = -2$	$T_2[2,6,0,5,2] = 1$	$T_2[2,6,1,2,4] = 2$
$T_2[2,6,1,4,2] = -1$	$T_2[2,6,2,0,5] = 1$	$T_2[2,6,2,1,4] = -1$
$T_2[2,6,2,2,3] = -1$	$T_2[2,6,2,3,2] = 2$	$T_2[2,6,2,4,1] = -1$
$T_2[2,6,2,5,0] = 1$	$T_2[2,6,3,2,2] = -1$	$T_2[2,6,4,1,2] = -1$
$T_2[2,6,4,2,1] = 2$	$T_2[2,6,5,0,2] = 1$	$T_2[2,6,5,2,0] = -2$
$T_2[3,0,3,5,6] = -2$	$T_2[3,0,3,6,5] = 1$	$T_2[3,0,5,3,6] = 1$
$T_2[3,0,5,6,3] = 1$	$T_2[3,0,6,3,5] = 1$	$T_2[3,0,6,5,3] = -2$
$T_2[3,1,3,4,6] = 2$	$T_2[3,1,3,6,4] = -1$	$T_2[3,1,4,3,6] = -1$
$T_2[3,1,4,6,3] = -1$	$T_2[3,1,6,3,4] = -1$	$T_2[3,1,6,4,3] = 2$
$T_2[3,2,3,3,6] = -1$	$T_2[3,2,3,6,3] = 2$	$T_2[3,2,6,3,3] = -1$
$T_2[3,3,0,5,6] = 1$	$T_2[3,3,0,6,5] = -2$	$T_2[3,3,1,4,6] = -1$
$T_2[3,3,1,6,4] = 2$	$T_2[3,3,2,3,6] = 2$	$T_2[3,3,2,6,3] = -1$

$T_2[3,3,3,2,6] = -1$	$T_2[3,3,3,6,2] = -1$	$T_2[3,3,4,1,6] = -1$
$T_2[3,3,4,6,1] = 2$	$T_2[3,3,5,0,6] = 1$	$T_2[3,3,5,6,0] = -2$
$T_2[3,3,6,0,5] = 1$	$T_2[3,3,6,1,4] = -1$	$T_2[3,3,6,2,3] = -1$
$T_2[3,3,6,3,2] = 2$	$T_2[3,3,6,4,1] = -1$	$T_2[3,3,6,5,0] = 1$
$T_2[3,4,1,3,6] = -1$	$T_2[3,4,1,6,3] = -1$	$T_2[3,4,3,1,6] = 2$
$T_2[3,4,3,6,1] = -1$	$T_2[3,4,6,1,3] = 2$	$T_2[3,4,6,3,1] = -1$
$T_2[3,5,0,3,6] = 1$	$T_2[3,5,0,6,3] = 1$	$T_2[3,5,3,0,6] = -2$
$T_2[3,5,3,6,0] = 1$	$T_2[3,5,6,0,3] = -2$	$T_2[3,5,6,3,0] = 1$
$T_2[3,6,0,3,5] = -2$	$T_2[3,6,0,5,3] = 1$	$T_2[3,6,1,3,4] = 2$
$T_2[3,6,1,4,3] = -1$	$T_2[3,6,2,3,3] = -1$	$T_2[3,6,3,0,5] = 1$
$T_2[3,6,3,1,4] = -1$	$T_2[3,6,3,2,3] = 2$	$T_2[3,6,3,3,2] = -1$
$T_2[3,6,3,4,1] = -1$	$T_2[3,6,3,5,0] = 1$	$T_2[3,6,4,1,3] = -1$
$T_2[3,6,4,3,1] = 2$	$T_2[3,6,5,0,3] = 1$	$T_2[3,6,5,3,0] = -2$
$T_2[4,0,4,5,6] = -2$	$T_2[4,0,4,6,5] = 1$	$T_2[4,0,5,4,6] = 1$
$T_2[4,0,5,6,4] = 1$	$T_2[4,0,6,4,5] = 1$	$T_2[4,0,6,5,4] = -2$
$T_2[4,1,4,4,6] = 1$	$T_2[4,1,4,6,4] = -2$	$T_2[4,1,6,4,4] = 1$
$T_2[4,2,3,4,6] = 1$	$T_2[4,2,3,6,4] = 1$	$T_2[4,2,4,3,6] = -2$
$T_2[4,2,4,6,3] = 1$	$T_2[4,2,6,3,4] = -2$	$T_2[4,2,6,4,3] = 1$
$T_2[4,3,2,4,6] = 1$	$T_2[4,3,2,6,4] = 1$	$T_2[4,3,4,2,6] = -2$
$T_2[4,3,4,6,2] = 1$	$T_2[4,3,6,2,4] = -2$	$T_2[4,3,6,4,2] = 1$
$T_2[4,4,0,5,6] = 1$	$T_2[4,4,0,6,5] = -2$	$T_2[4,4,1,4,6] = -2$
$T_2[4,4,1,6,4] = 1$	$T_2[4,4,2,3,6] = 1$	$T_2[4,4,2,6,3] = -2$
$T_2[4,4,3,2,6] = 1$	$T_2[4,4,3,6,2] = -2$	$T_2[4,4,4,1,6] = 1$
$T_2[4,4,4,6,1] = 1$	$T_2[4,4,5,0,6] = 1$	$T_2[4,4,5,6,0] = -2$
$T_2[4,4,6,0,5] = 1$	$T_2[4,4,6,1,4] = 1$	$T_2[4,4,6,2,3] = 1$
$T_2[4,4,6,3,2] = 1$	$T_2[4,4,6,4,1] = -2$	$T_2[4,4,6,5,0] = 1$
$T_2[4,5,0,4,6] = 1$	$T_2[4,5,0,6,4] = 1$	$T_2[4,5,4,0,6] = -2$
$T_2[4,5,4,6,0] = 1$	$T_2[4,5,6,0,4] = -2$	$T_2[4,5,6,4,0] = 1$
$T_2[4,6,0,4,5] = -2$	$T_2[4,6,0,5,4] = 1$	$T_2[4,6,1,4,4] = 1$
$T_2[4,6,2,3,4] = 1$	$T_2[4,6,2,4,3] = -2$	$T_2[4,6,3,2,4] = 1$
$T_2[4,6,3,4,2] = -2$	$T_2[4,6,4,0,5] = 1$	$T_2[4,6,4,1,4] = -2$
$T_2[4,6,4,2,3] = 1$	$T_2[4,6,4,3,2] = 1$	$T_2[4,6,4,4,1] = 1$
$T_2[4,6,4,5,0] = 1$	$T_2[4,6,5,0,4] = 1$	$T_2[4,6,5,4,0] = -2$
$T_2[5,0,5,5,6] = -1$	$T_2[5,0,5,6,5] = 2$	$T_2[5,0,6,5,5] = -1$
$T_2[5,1,4,5,6] = -1$	$T_2[5,1,4,6,5] = -1$	$T_2[5,1,5,4,6] = 2$
$T_2[5,1,5,6,4] = -1$	$T_2[5,1,6,4,5] = 2$	$T_2[5,1,6,5,4] = -1$
$T_2[5,2,3,5,6] = 1$	$T_2[5,2,3,6,5] = 1$	$T_2[5,2,5,3,6] = -2$
$T_2[5,2,5,6,3] = 1$	$T_2[5,2,6,3,5] = -2$	$T_2[5,2,6,5,3] = 1$
$T_2[5,3,2,5,6] = 1$	$T_2[5,3,2,6,5] = 1$	$T_2[5,3,5,2,6] = -2$
$T_2[5,3,5,6,2] = 1$	$T_2[5,3,6,2,5] = -2$	$T_2[5,3,6,5,2] = 1$
$T_2[5,4,1,5,6] = -1$	$T_2[5,4,1,6,5] = -1$	$T_2[5,4,5,1,6] = 2$
$T_2[5,4,5,6,1] = -1$	$T_2[5,4,6,1,5] = 2$	$T_2[5,4,6,5,1] = -1$
$T_2[5,5,0,5,6] = 2$	$T_2[5,5,0,6,5] = -1$	$T_2[5,5,1,4,6] = -1$
$T_2[5,5,1,6,4] = 2$	$T_2[5,5,2,3,6] = 1$	$T_2[5,5,2,6,3] = -2$
$T_2[5,5,3,2,6] = 1$	$T_2[5,5,3,6,2] = -2$	$T_2[5,5,4,1,6] = -1$
$T_2[5,5,4,6,1] = 2$	$T_2[5,5,5,0,6] = -1$	$T_2[5,5,5,6,0] = -1$
$T_2[5,5,6,0,5] = -1$	$T_2[5,5,6,1,4] = -1$	$T_2[5,5,6,2,3] = 1$
$T_2[5,5,6,3,2] = 1$	$T_2[5,5,6,4,1] = -1$	$T_2[5,5,6,5,0] = 2$
$T_2[5,6,0,5,5] = -1$	$T_2[5,6,1,4,5] = -1$	$T_2[5,6,1,5,4] = 2$
$T_2[5,6,2,3,5] = 1$	$T_2[5,6,2,5,3] = -2$	$T_2[5,6,3,2,5] = 1$
$T_2[5,6,3,5,2] = -2$	$T_2[5,6,4,1,5] = -1$	$T_2[5,6,4,5,1] = 2$
$T_2[5,6,5,0,5] = 2$	$T_2[5,6,5,1,4] = -1$	$T_2[5,6,5,2,3] = 1$
$T_2[5,6,5,3,2] = 1$	$T_2[5,6,5,4,1] = -1$	$T_2[5,6,5,5,0] = -1$

TABLE III: Tensor T_2 (multiplied by $12\sqrt{5}$).

$T_3[0,0,0,5,6] = -1$	$T_3[0,0,0,6,5] = 1$	$T_3[0,0,1,4,6] = 1$
$T_3[0,0,2,3,6] = -1$	$T_3[0,0,3,2,6] = -1$	$T_3[0,0,4,1,6] = 1$
$T_3[0,0,5,6,0] = -1$	$T_3[0,0,6,1,4] = -1$	$T_3[0,0,6,2,3] = 1$
$T_3[0,0,6,3,2] = 1$	$T_3[0,0,6,4,1] = -1$	$T_3[0,0,6,5,0] = 1$
$T_3[0,1,0,6,4] = -1$	$T_3[0,1,4,0,6] = -1$	$T_3[0,1,4,6,0] = 1$
$T_3[0,1,6,0,4] = 1$	$T_3[0,2,0,6,3] = 1$	$T_3[0,2,3,0,6] = 1$
$T_3[0,2,3,6,0] = -1$	$T_3[0,2,6,0,3] = -1$	$T_3[0,3,0,6,2] = 1$
$T_3[0,3,2,0,6] = 1$	$T_3[0,3,2,6,0] = -1$	$T_3[0,3,6,0,2] = -1$
$T_3[0,4,0,6,1] = -1$	$T_3[0,4,1,0,6] = -1$	$T_3[0,4,1,6,0] = 1$
$T_3[0,4,6,0,1] = 1$	$T_3[0,5,0,0,6] = 1$	$T_3[0,5,6,0,0] = -1$
$T_3[0,6,0,0,5] = -1$	$T_3[0,6,0,1,4] = 1$	$T_3[0,6,0,2,3] = -1$
$T_3[0,6,0,3,2] = -1$	$T_3[0,6,0,4,1] = 1$	$T_3[0,6,1,4,0] = -1$
$T_3[0,6,2,3,0] = 1$	$T_3[0,6,3,2,0] = 1$	$T_3[0,6,4,1,0] = -1$
$T_3[0,6,5,0,0] = 1$	$T_3[1,0,1,6,5] = 1$	$T_3[1,0,5,1,6] = 1$
$T_3[1,0,5,6,1] = -1$	$T_3[1,0,6,1,5] = -1$	$T_3[1,1,0,5,6] = -1$
$T_3[1,1,1,4,6] = 1$	$T_3[1,1,1,6,4] = -1$	$T_3[1,1,2,3,6] = -1$
$T_3[1,1,3,2,6] = -1$	$T_3[1,1,4,6,1] = 1$	$T_3[1,1,5,0,6] = -1$
$T_3[1,1,6,0,5] = 1$	$T_3[1,1,6,2,3] = 1$	$T_3[1,1,6,3,2] = 1$
$T_3[1,1,6,4,1] = -1$	$T_3[1,1,6,5,0] = 1$	$T_3[1,2,1,6,3] = 1$
$T_3[1,2,3,1,6] = 1$	$T_3[1,2,3,6,1] = -1$	$T_3[1,2,6,1,3] = -1$
$T_3[1,3,1,6,2] = 1$	$T_3[1,3,2,1,6] = 1$	$T_3[1,3,2,6,1] = -1$
$T_3[1,3,6,1,2] = -1$	$T_3[1,4,1,1,6] = -1$	$T_3[1,4,6,1,1] = 1$
$T_3[1,5,0,1,6] = 1$	$T_3[1,5,0,6,1] = -1$	$T_3[1,5,1,6,0] = 1$
$T_3[1,5,6,1,0] = -1$	$T_3[1,6,0,5,1] = 1$	$T_3[1,6,1,0,5] = -1$
$T_3[1,6,1,1,4] = 1$	$T_3[1,6,1,2,3] = -1$	$T_3[1,6,1,3,2] = -1$
$T_3[1,6,1,5,0] = -1$	$T_3[1,6,2,3,1] = 1$	$T_3[1,6,3,2,1] = 1$
$T_3[1,6,4,1,1] = -1$	$T_3[1,6,5,0,1] = 1$	$T_3[2,0,2,6,5] = 1$
$T_3[2,0,5,2,6] = 1$	$T_3[2,0,5,6,2] = -1$	$T_3[2,0,6,2,5] = -1$
$T_3[2,1,2,6,4] = -1$	$T_3[2,1,4,2,6] = -1$	$T_3[2,1,4,6,2] = 1$
$T_3[2,1,6,2,4] = 1$	$T_3[2,2,0,5,6] = -1$	$T_3[2,2,1,4,6] = 1$
$T_3[2,2,2,3,6] = -1$	$T_3[2,2,2,6,3] = 1$	$T_3[2,2,3,6,2] = -1$
$T_3[2,2,4,1,6] = 1$	$T_3[2,2,5,0,6] = -1$	$T_3[2,2,6,0,5] = 1$
$T_3[2,2,6,1,4] = -1$	$T_3[2,2,6,3,2] = 1$	$T_3[2,2,6,4,1] = -1$
$T_3[2,2,6,5,0] = 1$	$T_3[2,3,2,2,6] = 1$	$T_3[2,3,6,2,2] = -1$
$T_3[2,4,1,2,6] = -1$	$T_3[2,4,1,6,2] = 1$	$T_3[2,4,2,6,1] = -1$
$T_3[2,4,6,2,1] = 1$	$T_3[2,5,0,2,6] = 1$	$T_3[2,5,0,6,2] = -1$
$T_3[2,5,2,6,0] = 1$	$T_3[2,5,6,2,0] = -1$	$T_3[2,6,0,5,2] = 1$
$T_3[2,6,1,4,2] = -1$	$T_3[2,6,2,0,5] = -1$	$T_3[2,6,2,1,4] = 1$
$T_3[2,6,2,2,3] = -1$	$T_3[2,6,2,4,1] = 1$	$T_3[2,6,2,5,0] = -1$
$T_3[2,6,3,2,2] = 1$	$T_3[2,6,4,1,2] = -1$	$T_3[2,6,5,0,2] = 1$
$T_3[3,0,3,6,5] = 1$	$T_3[3,0,5,3,6] = 1$	$T_3[3,0,5,6,3] = -1$
$T_3[3,0,6,3,5] = -1$	$T_3[3,1,3,6,4] = -1$	$T_3[3,1,4,3,6] = -1$
$T_3[3,1,4,6,3] = 1$	$T_3[3,1,6,3,4] = 1$	$T_3[3,2,3,3,6] = 1$
$T_3[3,2,6,3,3] = -1$	$T_3[3,3,0,5,6] = -1$	$T_3[3,3,1,4,6] = 1$
$T_3[3,3,2,6,3] = -1$	$T_3[3,3,3,2,6] = -1$	$T_3[3,3,3,6,2] = 1$
$T_3[3,3,4,1,6] = 1$	$T_3[3,3,5,0,6] = -1$	$T_3[3,3,6,0,5] = 1$
$T_3[3,3,6,1,4] = -1$	$T_3[3,3,6,2,3] = 1$	$T_3[3,3,6,4,1] = -1$
$T_3[3,3,6,5,0] = 1$	$T_3[3,4,1,3,6] = -1$	$T_3[3,4,1,6,3] = 1$
$T_3[3,4,3,6,1] = -1$	$T_3[3,4,6,3,1] = 1$	$T_3[3,5,0,3,6] = 1$
$T_3[3,5,0,6,3] = -1$	$T_3[3,5,3,6,0] = 1$	$T_3[3,5,6,3,0] = -1$
$T_3[3,6,0,5,3] = 1$	$T_3[3,6,1,4,3] = -1$	$T_3[3,6,2,3,3] = 1$
$T_3[3,6,3,0,5] = -1$	$T_3[3,6,3,1,4] = 1$	$T_3[3,6,3,3,2] = -1$
$T_3[3,6,3,4,1] = 1$	$T_3[3,6,3,5,0] = -1$	$T_3[3,6,4,1,3] = -1$
$T_3[3,6,5,0,3] = 1$	$T_3[4,0,4,6,5] = 1$	$T_3[4,0,5,4,6] = 1$
$T_3[4,0,5,6,4] = -1$	$T_3[4,0,6,4,5] = -1$	$T_3[4,1,4,4,6] = -1$
$T_3[4,1,6,4,4] = 1$	$T_3[4,2,3,4,6] = 1$	$T_3[4,2,3,6,4] = -1$
$T_3[4,2,4,6,3] = 1$	$T_3[4,2,6,4,3] = -1$	$T_3[4,3,2,4,6] = 1$
$T_3[4,3,2,6,4] = -1$	$T_3[4,3,4,6,2] = 1$	$T_3[4,3,6,4,2] = -1$
$T_3[4,4,0,5,6] = -1$	$T_3[4,4,1,6,4] = 1$	$T_3[4,4,2,3,6] = -1$
$T_3[4,4,3,2,6] = -1$	$T_3[4,4,4,1,6] = 1$	$T_3[4,4,4,6,1] = -1$
$T_3[4,4,5,0,6] = -1$	$T_3[4,4,6,0,5] = 1$	$T_3[4,4,6,1,4] = -1$
$T_3[4,4,6,2,3] = 1$	$T_3[4,4,6,3,2] = 1$	$T_3[4,4,6,5,0] = 1$
$T_3[4,5,0,4,6] = 1$	$T_3[4,5,0,6,4] = -1$	$T_3[4,5,4,6,0] = 1$
$T_3[4,5,6,4,0] = -1$	$T_3[4,6,0,5,4] = 1$	$T_3[4,6,1,4,4] = -1$
$T_3[4,6,2,3,4] = 1$	$T_3[4,6,3,2,4] = 1$	$T_3[4,6,4,0,5] = -1$
$T_3[4,6,4,2,3] = -1$	$T_3[4,6,4,3,2] = -1$	$T_3[4,6,4,4,1] = 1$
$T_3[4,6,4,5,0] = -1$	$T_3[4,6,5,0,4] = 1$	$T_3[5,0,5,5,6] = 1$
$T_3[5,0,6,5,5] = -1$	$T_3[5,1,4,5,6] = -1$	$T_3[5,1,4,6,5] = 1$
$T_3[5,1,5,6,4] = -1$	$T_3[5,1,6,5,4] = 1$	$T_3[5,2,3,5,6] = 1$
$T_3[5,2,3,6,5] = -1$	$T_3[5,2,5,6,3] = 1$	$T_3[5,2,6,5,3] = -1$
$T_3[5,3,2,5,6] = 1$	$T_3[5,3,2,6,5] = -1$	$T_3[5,3,5,6,2] = 1$

$T_3[5,3,6,5,2] = -1$	$T_3[5,4,1,5,6] = -1$	$T_3[5,4,1,6,5] = 1$	$T_3[5,6,1,4,5] = -1$	$T_3[5,6,2,3,5] = 1$	$T_3[5,6,3,2,5] = 1$
$T_3[5,4,5,6,1] = -1$	$T_3[5,4,6,5,1] = 1$	$T_3[5,5,0,6,5] = -1$	$T_3[5,6,4,1,5] = -1$	$T_3[5,6,5,1,4] = 1$	$T_3[5,6,5,2,3] = -1$
$T_3[5,5,1,4,6] = 1$	$T_3[5,5,2,3,6] = -1$	$T_3[5,5,3,2,6] = -1$	$T_3[5,6,5,3,2] = -1$	$T_3[5,6,5,4,1] = 1$	$T_3[5,6,5,5,0] = -1$
$T_3[5,5,4,1,6] = 1$	$T_3[5,5,5,0,6] = -1$	$T_3[5,5,5,6,0] = 1$			
$T_3[5,5,6,0,5] = 1$	$T_3[5,5,6,1,4] = -1$	$T_3[5,5,6,2,3] = 1$			
$T_3[5,5,6,3,2] = 1$	$T_3[5,5,6,4,1] = -1$	$T_3[5,6,0,5,5] = 1$			

TABLE IV: Tensor T_3 (multiplied by $4\sqrt{15}$).

[1] R. Orús and G. Vidal, "Simulation of two-dimensional quantum systems on an infinite lattice revisited: Corner transfer matrix for tensor contraction," Phys. Rev. B **80**, 094403 (2009).

[2] J. I. Cirac, D. Poilblanc, N. Schuch, and F. Verstraete, "Entanglement spectrum and boundary theories with projected entangled-pair states," Phys. Rev. B **83**, 245134 (2011).

[3] H.-C. Jiang, R. R. P. Singh, and L. Balents, "Accuracy of topological entanglement entropy on finite cylinders," Phys. Rev. Lett. **111**, 107205 (2013).

[4] H. Li and F. D. M. Haldane, "Entanglement Spectrum as a Generalization of Entanglement Entropy: Identification of Topological Order in Non-Abelian Fractional Quantum Hall Effect States," Physical Review Letters **101**, 010504 (2008).